



# The role of porosity in polyester microparticles for drug delivery<sup>☆</sup>

Simon Pöttgen<sup>a</sup>, Magdalena Mazurek-Budzyńska<sup>b</sup>, Christian Wischke<sup>a,\*</sup>

<sup>a</sup> Martin-Luther-University Halle-Wittenberg, Institute of Pharmacy, Kurt-Mothes-Str. 3 06120 Halle, Germany

<sup>b</sup> Warsaw University of Technology, Faculty of Chemistry, Noakowskiego 3 00-664 Warsaw, Poland

## ARTICLE INFO

### Keywords:

Microparticle  
Porosity  
Drug Carrier  
Pore closing  
Polylactide  
Poly(lactide-co-glycolide)

## ABSTRACT

Polymer microparticles are a cornerstone in the field of injectable sustained delivery systems: They allow the entrapment of various types of hydrophobic or hydrophilic drugs including biopharmaceuticals. Microparticles can be prepared from the material of choice and tailored to specific target sizes. Importantly, they can retain the drug at the local administration site to achieve a sustained drug release for long-term therapeutic effects. This review focuses on the role of porosity of microparticles as a tremendously important property. Principles to prepare porous carriers via different techniques and additives are discussed, emphasizing that porosity is not a static property but can be dynamic, e.g., for particles from polylactide or poly(lactide-co-glycolide). Considering the contribution of porosity in the overall assessment of drug carrier systems, as well as their manipulation/alteration post-production such as by pore closing, will enlarge the understanding of polymer microparticles as an important class of modern pharmaceutical dosage forms.

## 1. Introduction

Polymeric carriers made of synthetic polyesters such as polylactide (PLA), poly(lactide-co-glycolide) (PLGA), or poly( $\epsilon$ -caprolactone) (PCL) have not only become a standard technology in experimental research for controlled drug delivery (Espinoza et al., 2020; Su et al., 2021; Wischke and Schwendeman, 2008; Woodruff and Huttmacher, 2010), but are also frequently used in clinical practice as approved pharmaceutical products, e.g. in prostate cancer therapy. In principle, numerous active pharmaceutical ingredients (APIs) with various properties can be incorporated, covering a broad range from small hydrophobic molecules to larger substances like proteins or peptides (Lagrecia et al., 2020). However, simply encapsulating a compound is not sufficient; attention must also be given to drug integrity, encapsulation efficiency, drug release rates, and release profiles. In some cases, undesired phenomena such as burst release (Zhou et al., 2018) may be observable, suggesting unsuitable drug distribution in the particles or massive changes in particle structure. In other cases, release rates are very minor and release is incomplete (Janich et al., 2019), suggesting a lack of diffusion paths for water and dissolved APIs, a chemical alteration of drugs, and/or disadvantageous phase distribution coefficients.

To understand such phenomena, they must be linked to the causes of improper release profiles, and measures should be derived to improve

the formulation. Thus, it is necessary to understand microparticles in their full complexity: They are in most cases non-homogeneously sized objects that are typically produced by statistical events leading to a distribution of all relevant properties within each particle sample. Clearly, the physicochemical properties of the matrix polymer, the particle size, or the drug characteristics can be relevant to achieve certain drug loading or drug release properties (Han et al., 2016). However, another highly relevant parameter is particle porosity. Despite its obvious effects on encapsulation efficiency, diffusion pathways, and release kinetics of encapsulated drugs, particle porosity is rarely characterized and is sometimes only visually described.

According to the IUPAC, pore sizes can be classified into (i) micropores (<2 nm), (ii) mesopores (2–50 nm) and (iii) macropores (>50 nm) (Rouquerol et al., 1994). Typical pore sizes for porous PLGA and PLA particles are macroporous and can reach up to several  $\mu\text{m}$ . Porous microparticles can be produced by various fabrication techniques, including electrospraying (Gao et al., 2015), microfluidics (Amoyav and Benny, 2019), or emulsion-based methods (Crofts and Park, 1995; Shi et al., 2009; Wischke and Schwendeman, 2008). Pore-forming additives (“porogens”) are often used in these techniques to create voids within the polymer matrix through different mechanisms. Importantly, the fabricated pore structures must not be considered to be static. Pores have been shown to change their size and number in different time frames

<sup>☆</sup> This article is part of a special issue entitled: ‘Parenteral Time-Controlled Drug Delivery’ published in International Journal of Pharmaceutics.

\* Corresponding author.

E-mail address: [christian.wischke@pharmazie.uni-halle.de](mailto:christian.wischke@pharmazie.uni-halle.de) (C. Wischke).

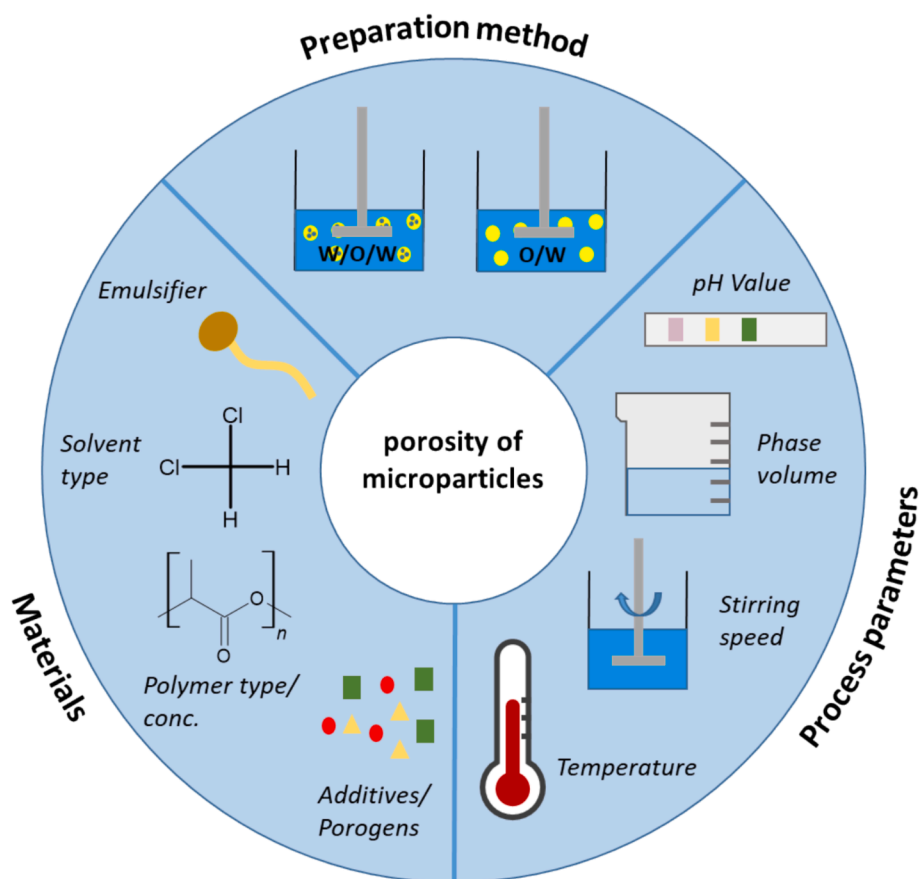


Fig. 1. Influence of different factors on the porosity of microparticles.

(Mazzara et al., 2013), thus affecting the exchange of solutes by diffusion into and out of the particle (Desai and Schwendeman, 2013; Huang et al., 2015; Wang et al., 2002).

This review focuses on the role of porosity in enhancing the performance of microparticles as drug carriers. The manufacturing process of porous particles using emulsion-based techniques is explored in detail, with emphasis on how process parameters – such as mixing conditions and solvent exchange – as well as the formulation – such as emulsifier concentrations and the specific type of polymer used as matrix material – can impact particle porosity. In addition, the use of porogens (gas-forming agents, osmotic agents, and extractable compounds) to induce porosity is systematically analyzed, alongside their effects on pore sizes and particle characteristics. Furthermore, methods to quantitatively characterize porosity are briefly presented. Eventually, the review highlights dynamics in pore structures, including pore opening and closing mechanisms, their use for self-encapsulation strategies, and the potential impact on sustained drug release. A deeper understanding of these processes will enable more effective tailoring of drug release kinetics, making porous polyester microparticles a versatile tool for controlled drug delivery.

It must be noted that there will be no general judgment of certain pore structures as better or worse in this article, e.g. small versus large pores or higher versus lower porosity. Application needs linked e.g. to desired release kinetics or drug properties will be mandatory to define a proper specification for porous particles.

## 2. Fabrication of microparticles with control of porosity

Pores in microparticles can be created by certain process characteristics (e.g. interfaces generated by stirring, extraction rate, etc.) and by the nature and relative composition of the employed materials (e.g. type

and concentration of polymer, addition of porogens, etc.) (Fig. 1).

In section 2, the most common preparation method for porous particles is introduced including relevant process parameters, material characteristics, etc. In section 3, there is a focus on different categories of porogens and the underlying principle of pore formation, also illustrating that porogens may be useful additives for different types of preparation techniques.

### 2.1. Emulsion-based methods

Emulsion-based techniques are the most commonly used methods for the fabrication of both porous and nonporous microparticles. The easy setup and the flexibility to widely modify fabrication protocols (solvent type, phase volumes, stirring equipment, additives, etc...) justify their extensive use, particularly in academic research. Depending on polymer and drug properties, different phase types (o/w, s/o/w, w/o/w, o/o; o: organic/oil, w: aqueous, s: suspended solid) of emulsions can be facilitated for successful encapsulation of different compounds. However, o/w and w/o/w emulsions are predominantly used due to their simplicity and comparatively high encapsulation efficiency of lipophilic or hydrophilic molecules, respectively (Wischke and Schwendeman, 2008). For instance, an o/w emulsion may consist of an organic solvent (o-phase) such as methylene chloride containing a dissolved matrix-forming polymer, which is dispersed in an outer water phase (w) supplemented with an appropriate emulsifier like poly(vinyl alcohol) (PVA).

#### 2.1.1. Choice of emulsion type and influence of phase volume

The choice of the emulsion type is typically driven by drug properties, as for high encapsulation efficiencies the drug shall, in many cases, be dissolved either in the o-phase (o/w) or in a  $w_1$  water phase ( $w_1/o$ )

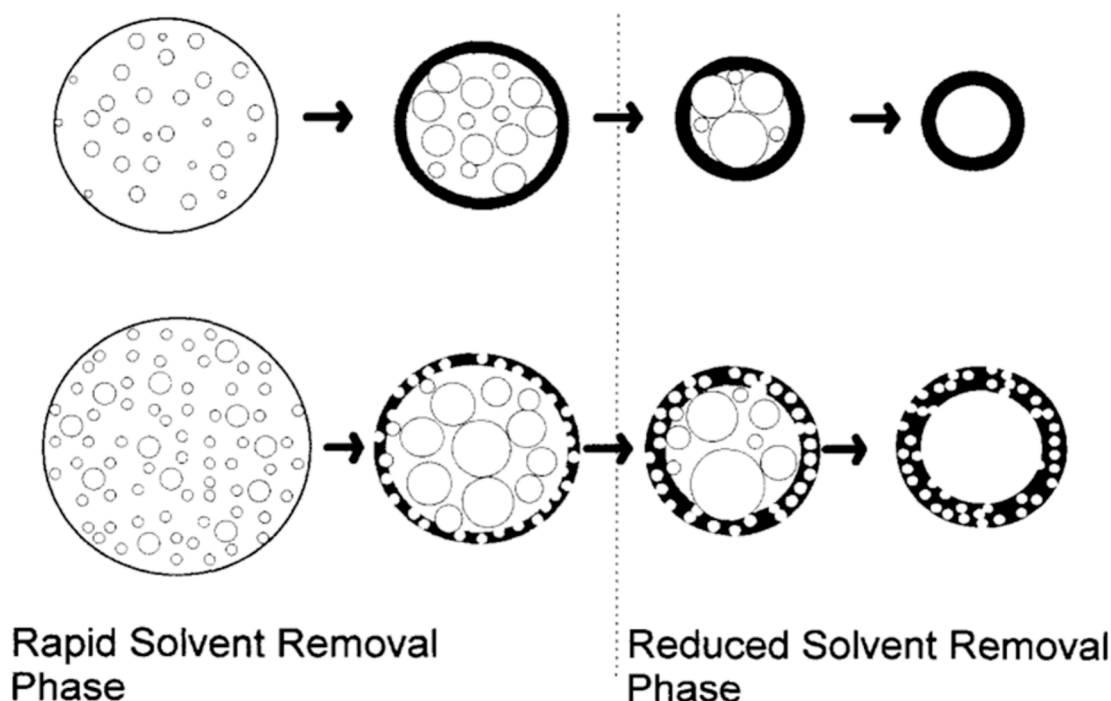


Fig. 2. Solvent removal process and polymer solidification of PLGA particles with lower (upper panel) and higher  $w_1$  phase volume (lower panel). Reprinted from (Crotts and Park, 1995) with permission from Elsevier.

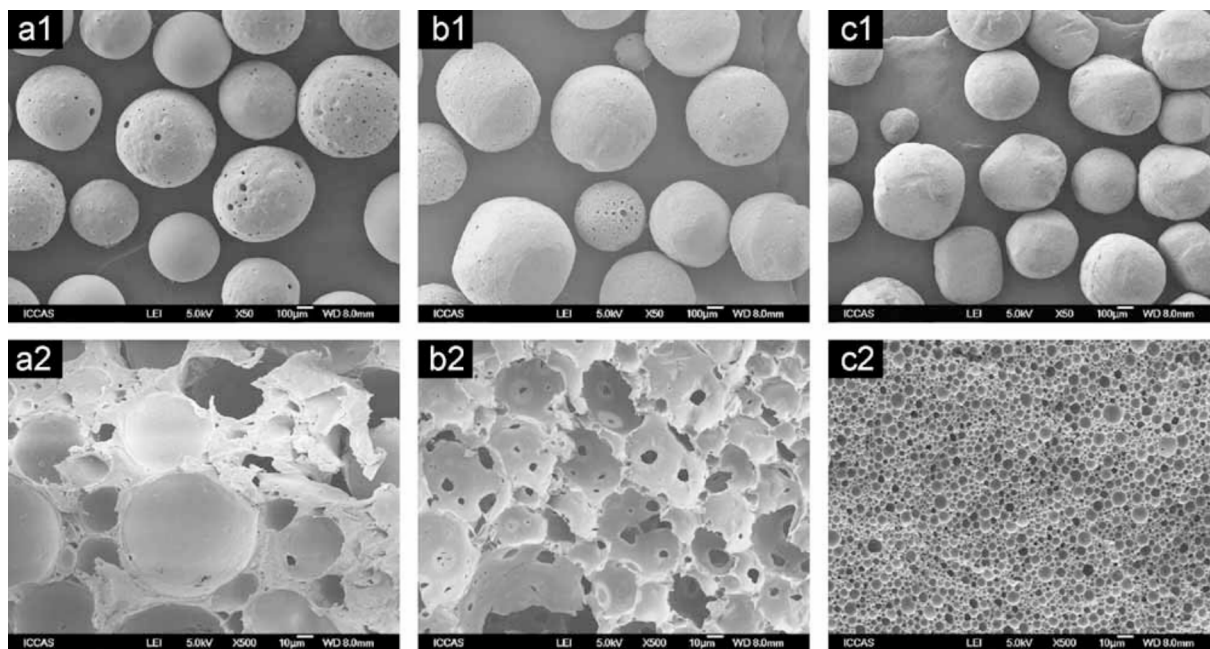
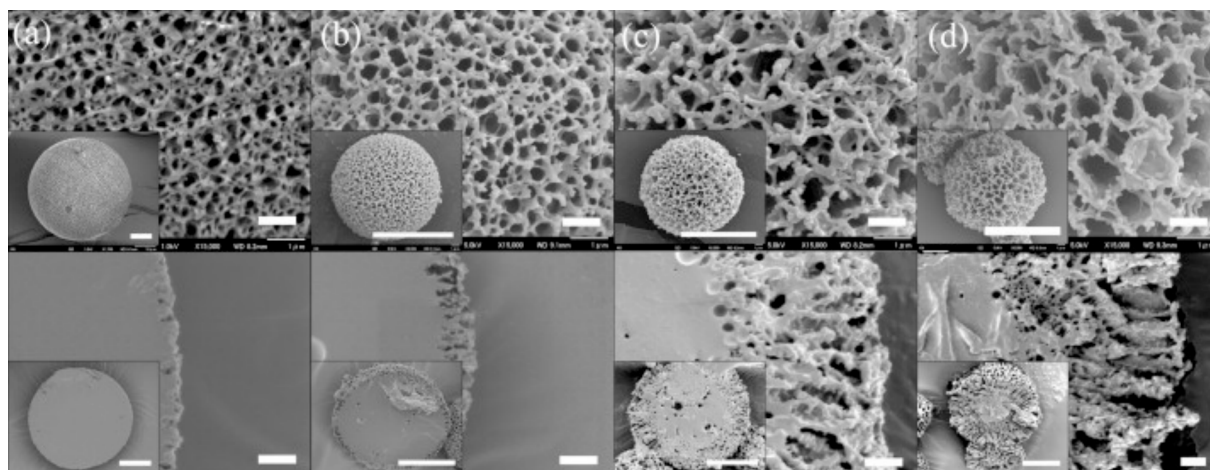


Fig. 3. Effect of homogenization speed of the primary emulsion on particle porosity. SEM images of the surface (a1, b1, and c1) and cross-section (a2, b2, and c2) of PLA microspheres whose primary emulsion was emulsified by a homogenizer at the speed of about a) 8 000, b) 11 500, and c) 30 000 rpm. Fabrication conditions:  $w_1$  phase: 1.25 mL of a 5 %  $\text{NH}_4\text{HCO}_3$  solution; Oil phase: 4 mL of a 6.25 % PLA/ $\text{CH}_2\text{Cl}_2$  solution;  $w_2$  phase: 150 mL of a 0.1 % PVA solution. The secondary emulsion ( $(w_1/o)/w_2$ ) was emulsified by an impeller at 200 rpm for 4 h. Reprinted from (Shi et al., 2009) with permission from Wiley.

$w_2$ ). However, the emulsion type can be a decisive parameter to create porosity. In particular,  $w/o/w$  emulsions are expected to increase particle porosity as aqueous  $w_1$  droplets are introduced in the polymer phase. For instance, the  $o/w$  method can lead to particles with nonporous surfaces, while increasing volume ratios of  $w_1$  to  $o$ -phases provided particles with one (hollow capsule) or several inner cavities (Crotts and Park, 1995). Interesting ultrastructures of the core and shell were

reported for PLGA microcapsules, having either a porous or a nonporous surface layer (Fig. 2). The authors concluded that higher  $w_1$  phase volumes cause the inclusion of aqueous droplets in the solidifying skin layer and result in a porous shell (Crotts and Park, 1995). Similar findings of higher porosity (Mao et al., 2007) and larger pore sizes with increasing volume of  $w_1$  have been confirmed for PLGA (Cui et al., 2005; Liu et al., 2006; Mao et al., 2007; Schlicher et al., 1997) and PCL (Yang



**Fig. 4.** Effect of stirring rates on the ultrastructure of PLGA microparticles incorporating dispersed hydroxyapatite. Surface (top row) and cross-sectional (bottom row) images of particles prepared at stirring rates of a) 195, b) 270, c) 300, or d) 375 rpm. Scale bars are 10  $\mu\text{m}$  (insets) and 1  $\mu\text{m}$  (detailed view), respectively. Reprinted from (Takai et al., 2011) with permission from Elsevier.

et al., 2001). Obviously, it is also important to produce very small droplet sizes of the  $w_1$  phase with good  $w_1$  droplet stability, especially if the primary  $w_1$  droplets are used to directly template individual pores. Moreover, it should be considered that hydrophilic drugs, additives, and salts dissolved in  $w_1$  may dominate the pore formation by osmotic principles rather than having the individual  $w_1$  volumes defining the final pore volumes (see section 3).

In addition to the  $w_1/o$  ratios of double emulsion, the outer  $w_2$  water phase is yet another known parameter affecting particle characteristics. While a direct impact of  $w_2$  volumes on particle sizes (due to changes in solidification speed and solvent removal) is established (Wischke and Schwendeman, 2008), there is less literature on its effect on porosity. One study prepared PLGA particles with increasing  $w_2$  volumes and found a slight decrease of internal porosity (15.83 – 11.81 %), while surface porosity slightly increased. A disruption of the skin layer by drug loss could be the reason for the increased surface porosity with the higher  $w_2$  volumes as indicated by a simultaneous decrease of the encapsulation efficiency (Mao et al., 2007). Another study on PLGA particles found that pore sizes reached a plateau when the ratio of  $w_2$  to  $o$  volumes exceeded a certain threshold, in this case being 15:1 (Si et al., 2021).

Overall, in addition to phase volumes and volume ratios, other parameters that interfere with solidification speed and solvent removal rates will need to be taken into account, such as water solubility of the  $o$ -phase solvent, gas exchange at the  $w_2$ -air interface and further factors (polymer concentration, emulsification procedure, additives).

### 2.1.2. Emulsification technique

It is mandatory to use stirring and homogenization equipment for the production of microparticles in order to obtain homogenous emulsions which serve as templates for particles with narrow size distributions. The choice of stirring tools usually goes hand in hand with the choice of the emulsion types as mentioned above. Magnetic stirring is occasionally employed for crude  $o/w$  emulsions or for mild mixing during the solvent extraction/evaporation step. High-speed stirrers (e.g. Ultra-Turrax) are used for the primary  $w_1/o$  emulsion of  $w_1/o/w_2$  emulsions. The small droplet sizes obtained with high-speed stirrers can support the stability of the emulsion and reduce the coalescence of  $w_1$  droplets. This coalescence is typically undesired as it may result in a reduction of the drug encapsulation efficiency and/or create particles with large holes rather than a fine porous core structure.

A rise in the stirring speed of magnetic stirring as well as of high-speed stirring was shown to reduce pore sizes (Hong et al., 2005; Mao et al., 2007; Shi et al., 2009; Si et al., 2021). For instance, PLA

microparticles templated by an  $o/w$  emulsion with magnetic stirring showed a reduction of pore sizes from 24 to 12  $\mu\text{m}$  (along with a reduction of overall particle sizes) when the stirring speed was increased from 300 to 800 rpm (Hong et al., 2005). For particles prepared by the  $w_1/o/w_2$  technique, the stirring rates in the primary  $w_1/o$  emulsification had more influence on the pore sizes of the particle core than the high-speed stirring in the secondary ( $w_1/o$ )/ $w_2$  emulsification. The particle surface texture was not affected by this process variation (Fig. 3) (Mao et al., 2007; Shi et al., 2009).

The encapsulation of compounds can also be achieved when suspensions of drugs or other additives are added in the organic phase, leading to  $s/o/w$  dispersions. Hydroxyapatite-loaded PLGA particles were prepared via the  $s/o/w$  technique, where the pre-formed emulsion was added into a hardening bath. Intermediate stirring times of the  $s/o/w$  emulsion before addition to the hardening bath produced more open-porous particles (note: by contrast, short or long stirring produced fewer surface pores), while higher magnetic stirring rates at intermediate stirring times resulted in deeper and larger pores (Fig. 4). It was speculated that water enclosure in the  $o$ -phase of the nascent droplets and the stabilization of polymer-water interphases within the  $o$ -phase by dispersed hydroxyapatite resulted in the porous structure, since no porosity was observed in the absence of dispersed hydroxyapatite (Takai et al., 2011).

### 2.1.3. Choice of $o$ -phase solvent

Polymer solubility,  $o$ -phase viscosity, water-in-solvent solubility (void formation), and solvent-in-water solubility (extraction rates) – all are affected by the choice of solvent. A comparison of dichloromethane (DCM), chloroform, and ethyl acetate as the most commonly used solvents to prepare PLGA particles showed spherical shapes for DCM, more cubic particles from chloroform, or collapsed particles in the case of ethyl acetate (Amoyav and Benny, 2019). Non-spherical particles made with ethyl acetate were also obtained by other authors (Herrmann and Bodmeier, 1995b). Again, this may not be generalized considering the interplay of multiple parameters. Further authors prepared spherical and homogenous particles with chloroform and ethyl acetate (Shi et al., 2018).

It has been shown that using ethyl acetate for PLA particles resulted in hollow particles with a porous shell layer, but smooth surfaces (Shi et al., 2009). A similar structure was previously reported for PLGA particles (Wang et al., 2015). It has been discussed that polymer concentration (see also section 2.1.4), in addition to the selected organic solvent, affects particle morphology. For instance, doubling the PLGA concentration in ethyl acetate results in non-spherical, erythrocyte like



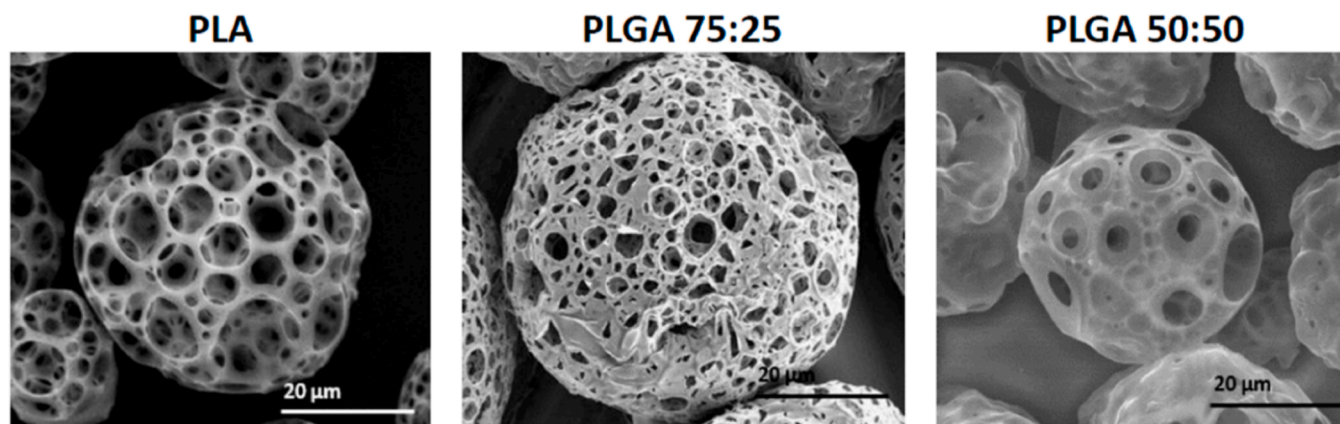


Fig. 5. Effect of copolymer composition on pore structures. SEM images showing porous microspheres obtained with PLA, PLGA 75:25 and PLGA 50:50. Adapted and reprinted from (Amoyav and Benny, 2019) with permission from MDPI under a Creative Commons Attribution 4.0 International License (<https://creativecommons.org/licenses/by/4.0/>).

particle structures.

The use of solvent mixtures is another concept to modulate mass transport processes. For instance, the o-phase can incorporate a polymer solvent in combination with co-solvents or non-solvents (for the polymer), which show a different volatility or solubility in the external phase than the main o-phase solvent. Supplementing DCM with *n*-hexane (a non-solvent for PLA) resulted in particles with a greater porosity and larger pore sizes. This effect was more pronounced with higher *n*-hexane levels due to accelerated phase separation (Hong et al., 2005).

#### 2.1.4. Polymer type and concentration

The selection of higher polymer concentrations is a common approach to modulate microparticle porosity as it increases the viscosity of the o-phase (Gaignaux et al., 2012; Wischke and Schwendeman, 2008), often resulting in smaller pores, lower overall porosity, and less open porous surfaces of microparticles (Hong et al., 2005; Kim and Sah, 2019; Mao et al., 2007; Reinhold and Schwendeman, 2013; Schlicher et al., 1997; Shi et al., 2009; Zhang et al., 2021). Still, it should be noted that a higher viscosity of the o-phase requires higher stirring speeds to obtain the same droplet/particle sizes (Wischke and Schwendeman, 2008). Furthermore, there may be functional limits, e.g., a too-high polymer concentration can hinder pore formation (and processability), while a too low concentrations can result in unstable and disrupted polymer matrices (Shi et al., 2009). Polymer concentration should therefore be evaluated as an important parameter for control of porosity and morphology (Kazazi-Hyseni et al., 2014).

Polymer characteristics (molecular weight, end groups, comonomers, etc.) can have a significant impact on the size and morphology of microparticles as well as their drug release pattern (Jalil and Nixon, 1990). In emulsion techniques with an outer aqueous phase (and potentially an additional inner aqueous phase), it can be expected that the diffusion of water into the organic polymer phase will be supported if the polymer provides excessive molecular motives for H-bonding (e.g. hydroxyl, ether, ester, amid groups). Therefore, the chemical nature of the polymer's repetitive units as well as the type and relative content of end groups (the latter depending on the molecular weight and potential branching) are of relevance.

According to a proposed concept, polymers with higher solubility in the respective o-phase solvent (i.e. typically polymers with lower molecular weights), take a longer time to reach their solubility limit during the solvent extraction/evaporation process and therefore may show higher porosity and higher drug leakage (lower encapsulation efficiencies) (Yeo and Park, 2004). Given the multi-parameter space that finally mediates pore formation, there are reports supporting this concept (Lee and Sah, 2016; Zhang et al., 2014), while other studies have contradictory observations (Cai et al., 2009; Schugens et al., 1994).

For example, when using 2-methylpentan as a porogen added to the o-phase, particles from 20 kDa PLGA were more porous than those from 50 kDa PLGA (Zhang et al., 2014). Higher porosity was also found for particles made from lower molecular weight PLGA, which were prepared by ammonolysis of the o-phase solvent isopropyl formate to isopropanol and formamide (non-solvents for PLGA; extractable into external water phase) (Lee and Sah, 2016). On the other hand, increasing the molecular weight of ester-endcapped and carboxyl-terminated PLGA by factor 3 (Resomer RG 502H vs. RG 503H) resulted in higher internal and surface porosity of particles (Cai et al., 2009). PLA particles prepared by w/o/w emulsification from PLA 60 kDa resulted in particles with a hollow core and small surface pore diameters, while PLA with extremely high molecular weight (840 kDa) showed more uniformly pore structures with bigger pore sizes both at the particle surface and within the core (Schugens et al., 1994). Importantly, this study also changed polymer concentrations to enable the processability of the otherwise too-viscous solutions of PLA 840 kDa. This emphasizes that the viscosity of the o-phase is yet another parameter of relevance. At a suitable o-phase viscosity, the o-phase is well dispersible and at the same time provides kinetic stabilization of  $w_1$  droplets in the primary emulsion to prevent them from coalescing.

In addition to the solubility of polymers in the o-phase solvent, their behavior at the oil-water interface can also be important in explaining particle formation. More specifically, low interaction of the polymer chains with water molecules will result in immediate polymer precipitation at the o/w or w/o interfaces forming a thin layer, which, in turn, may promote the stabilization and/or rigidification of these interfaces. PLA, compared to PLGA (the derivative with additional glycolide as a slightly more hydrophilic repetitive unit), created more porous particles due to faster interface solidification and particle hardening (Cui et al., 2005). The possible effect of the monomer composition of PLGAs (50:50 and 75:25 *rac*-lactide:glycolide content; molecular weights 40–75 kDa and 76–115 kDa, respectively) and PLA (100 % *rac*-lactide, 75–120 kDa) was illustrated by an increasing overall porosity and individual pore sizes with decreasing glycolide content in a set of formulations also containing a gas-forming porogen (Fig. 5) (Amoyav and Benny, 2019). The comparison of PLGA with carboxyl versus ethyl ester end groups showed that particles made by the w/o/w technique from PLGA-COOH had a low internal porosity but higher surface porosity. In contrast, the less hydrophilic PLGA with ethyl end caps better retained the  $w_1$  phase captured in the multivesicular microspheres (Mao et al., 2007). Another study based on w/o/w emulsions with porogens and mixed o-phase solvents showed similar results for ethyl capped PLGA, leading to smaller pores at a higher surface porosity and overall numbers of pores (Ni et al., 2017).

Composition effects of polymers may go beyond end groups and the

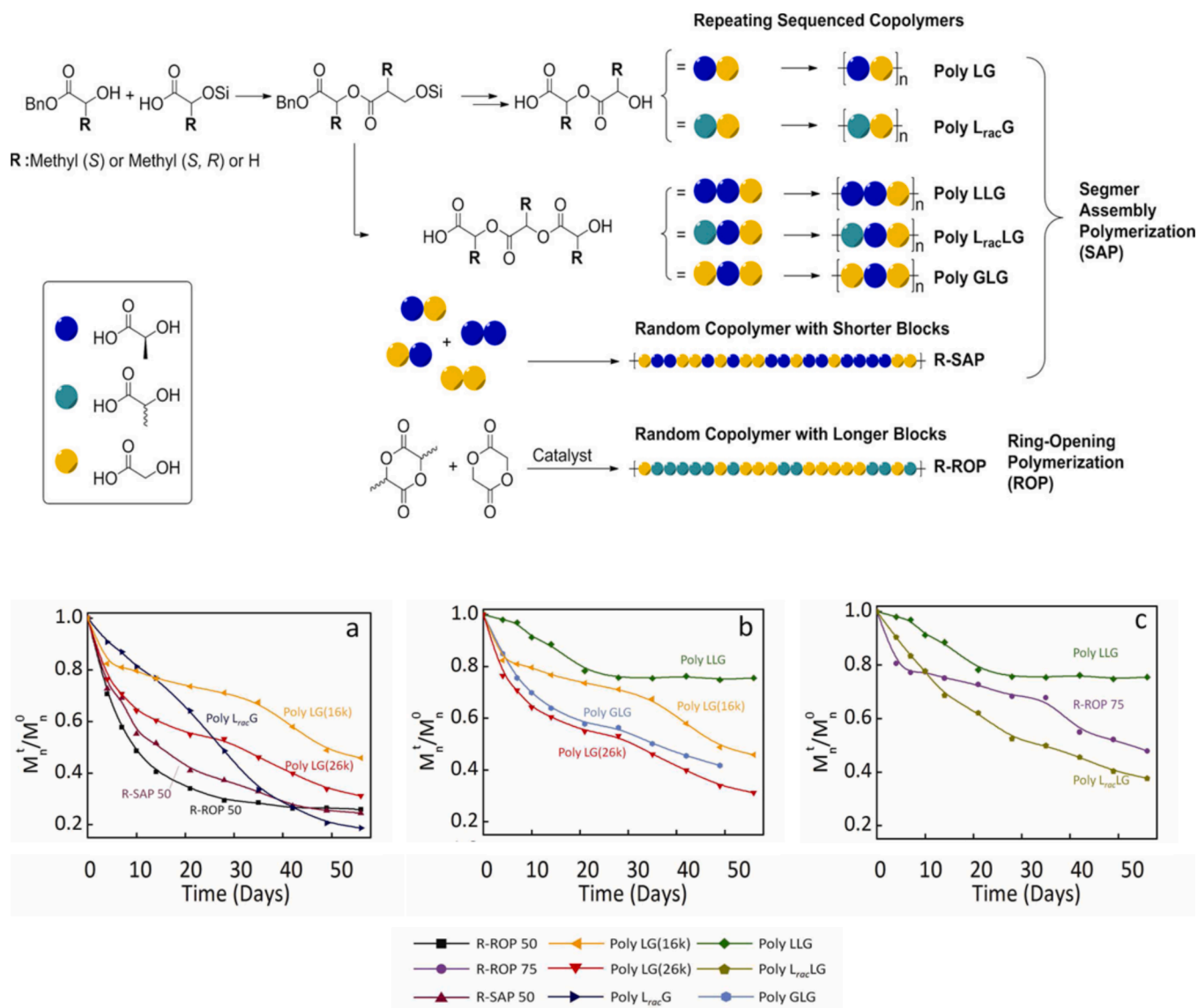


**Fig. 6.** Effect of PLGA sequence structure on material properties and degradation. (Top) Synthesis strategies to obtain PLGA copolymers with strictly repeating sequence structures or as random copolymers. (Bottom) Molecular weight loss as a function of hydrolytic degradation time for the repeating sequenced and random sequenced PLGAs: (a) comparison of all polymers with 50:50 LG ratio; (b) comparison of polymers with varying L:G ratios; (c) comparison of LLG polymers with varying stereochemistry. Adapted and reprinted with permission from (Li et al., 2012). Copyright © 2012, American Chemical Society.

content of standard comonomers. The tacticity of certain repetitive units with stereocenters, the sequence structure/ blockiness of statistical copolymers, defined block copolymer structures (e.g. A-B-A block copolymers) with different physicochemical properties of the blocks, or the use of certain types of linkers to connect polyester blocks e.g. to poly(ester-urethane)s – all can affect the ability of polymers to interact with water. While not directly comparable to conditions of much higher solvent diffusivity during particle preparation via emulsion techniques, long-term incubation of preformed microparticles from multi-block PLGA with urethane linkages revealed clearly higher water uptake than for standard PLGA (Mathew et al., 2015). Another study on electrospinning of PLGA-based poly(ester-urethane)s indicated some effects of the relative content and type of moieties of the urethane segments (aliphatic chains vs. additional fluorinated aromatic side groups) on the mass loss during degradation, which suggests different water influx rates (and hydrolysis rates) (Blakney et al., 2016). Given the broad spectrum of repetitive units that can be integrated into polyesters, e.g. those materials built by the condensation reaction of diols and diesters, longer hydrophilic segments or aliphatic vs. aromatic units may affect water

uptake (Wang et al., 2006). By introducing alternative comonomers in PLGA, such as trimethylene carbonate, it is not only possible to tailor mechanical properties (less relevant for microparticles than for implants), but also the interaction with water (Fan et al., 2019). Such differences observed during the aqueous incubation of dry polymers may potentially be transferable to water interaction during particle preparation in emulsion systems.

The effect of the sequence structure of PLGA on material properties was demonstrated to be highly relevant. Most existing PLGA raw materials are produced by ring-opening polymerization (ROP) from *rac*-dilactide and diglycolide (and are falsely labeled as poly(*D,L*-lactide-co-glycolide) instead of poly(*rac*-lactide-co-glycolide)). The ROP leads to a random copolymer structure with a certain blockiness depending on the employed catalysts. In such blocky PLGA, longer sequences of glycolide-glycolide linkages (weak links) will be attacked easier by water during degradation than lactide-glycolide linkages. In contrast, advanced synthesis techniques allow to produce PLGA with highly repetitive and defined sequence structures (Fig. 6) (Li et al., 2012; Li et al., 2011). While the authors did not study pore formation, the reported effects of

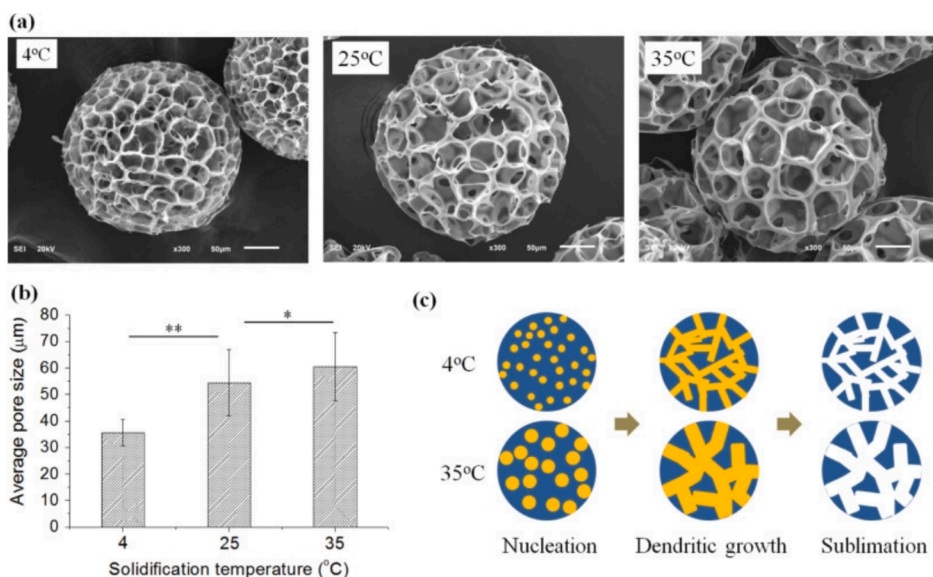


**Fig. 7.** Effect of temperature on pore formation mediated by a crystallizing porogen dissolved in the o-phase and later removed during lyophilization. (a) SEM morphologies of porous PCL microspheres with varying solidification temperatures (4, 25, and 35 °C) processed at fixed camphene content, sample, and sheath flow rates of 20 %, 1, and 15 ml/h, respectively. (Scale bar = 50 μm). (b) Average pore size increases steadily with increasing solidification temperature. (c) Schematic illustration of the proposed mechanism of how solidification temperature (degree of undercooling) affects the camphene nucleation and the resulting pore sizes. Reprinted from (Park et al., 2016) with permission from Elsevier.

monomer sequence on the degradation of these different types of PLGA copolymer microparticles are remarkable as a much higher mass loss was observable for the blocky random PLGA due to its enhanced interaction with water (Li et al., 2012; Li et al., 2011; Washington et al., 2017). Similar results were reported for poly(ester-urethane)s with either blocky or more homogeneous distributions of glycolide and  $\epsilon$ -caprolactone repetitive units in the soft segments, again showing faster degradation-induced pore formation and mass loss for the blocky materials presumably with additional contributions of microphase separation (Moghanizadeh-Ashkezari et al., 2018). Such observations might potentially be transferable to water-polymer interaction and thus pore formation during particle preparation by emulsion techniques.

### 2.1.5. Influence of emulsifier type and concentration

In most cases, it is mandatory to add emulsifiers to the continuous phase to prevent droplet coalescence during particle preparation or subsequent particle aggregation. Poly(vinyl alcohol) is the most commonly used emulsifier for PLGA particles because of its outstanding interaction with PLGA surfaces. With increasing emulsifier concentration, droplet size may decrease and surface perturbations (nascent pores) may potentially be stabilized better. For example, lower pore and particle size were reported for PLGA particles made by a double emulsion with increasing PVA concentration in the  $w_2$  phase (Sun et al., 2009). However, an overly high emulsifier concentration may not be desirable due to an increase of the viscosity of the continuous phase, high interface dynamics disturbing spherical droplet formation, undesired solubilisation of drug payloads leading to a leakage into the external phase, or potential toxicity of excess surfactants in a biological setting. In some cases, an increase of the PVA concentration in o/w emulsions led to larger pore sizes of PLA particles along with an overall size reduction of the particles (Hong et al., 2005).

In double emulsions, surfactants may also be used to stabilize the primary  $w_1/o$  emulsion. The addition of 2 % PVA to the inner water phase decreases pore sizes of PLGA particles significantly (Wang et al., 2015).

Just like the concentration of surfactants, the emulsifier properties are of central importance for a sufficient emulsion stability until particles eventually solidify. A series of studies investigated the effect of

increasing concentrations of the surface-active model payload bovine serum albumin (BSA) in the  $w_1$  phase, increasing concentrations of Poloxamer 188 in the o-phase, and combinations of both additives in the preparation of PLA and PLGA particles (Nihant et al., 1994, 1995; Schugens et al., 1994). An increase in BSA concentration, even in small quantities, had a positive effect on the stability of the primary emulsion (regardless of the used matrix polymer) and provided more uniform internal pore structures with smaller pore sizes. Poloxamer 188 (optimum 3 %) was shown to be less suitable for stabilizing  $w_1/o$  emulsions for PLGA particles efficiently as may be concluded from its HLB value (Nihant et al., 1995). For PLA particles, primary emulsion stability was supported by increasing concentrations of Poloxamer 188 only for selected (Schugens et al., 1994) but not all PLA materials. The complex effects that surfactant structure can have on porous particle formation are also represented in a study, which substituted the  $w_1$ -phase with PVA or BSA in order to obtain highly porous particles. In contrast, common surfactants, mainly non-ionic like Poloxamer 188 or Tween, provided particles without less pronounced surface pores and irregularly shaped particle surfaces (Bouissou et al., 2004).

In addition to widely established surfactants, also more recently introduced surface active molecules were investigated to stabilize polyester particles. For instance, based on a comparison of the use of PVA to D- $\alpha$ -tocopherol PEG succinate (TPGS) as a surfactant in the outer water phase of w/o/w emulsions for PLGA microparticle production, some authors claimed there was a more homogeneous particle size distribution for TPGS, despite this not being evident from the SEM images (Gaspar et al., 2015). TPGS is also frequently employed in nanoparticle preparation and may, if added to the o-phase at high concentrations, act as a porogen due to its hydrophilic PEG segment (Zhu et al., 2014). In another study with different surfactants (PVA, Tween 20, TPGS, star-shaped oligoethylene glycol partially functionalized with desamino tyrosine (sOEG-DAT)) used to stabilize oligopeptide nanoparticles (backbone with alternating amid and ester linkages), the provided SEM images do not allow for conclusions on porosity. However, it was obvious that only sOEG-DAT enabled a size control of the nanoparticles while e.g. TPGS failed to produce oligopeptide nanoparticles (Brunacci et al., 2017).



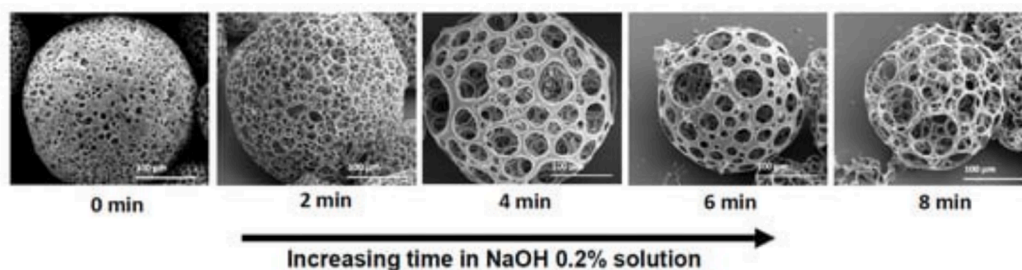


**Fig. 8.** Effect of NaOH posttreatment on PLGA microparticle porosity. SEM images of porous PLGA 75:25 microspheres at increased soaking time in NaOH 0.2 M solution. Reprinted from (Amoyav and Benny, 2019) with permission from MDPI under a Creative Commons Attribution 4.0 International License (<https://creativecommons.org/licenses/by/4.0/>).

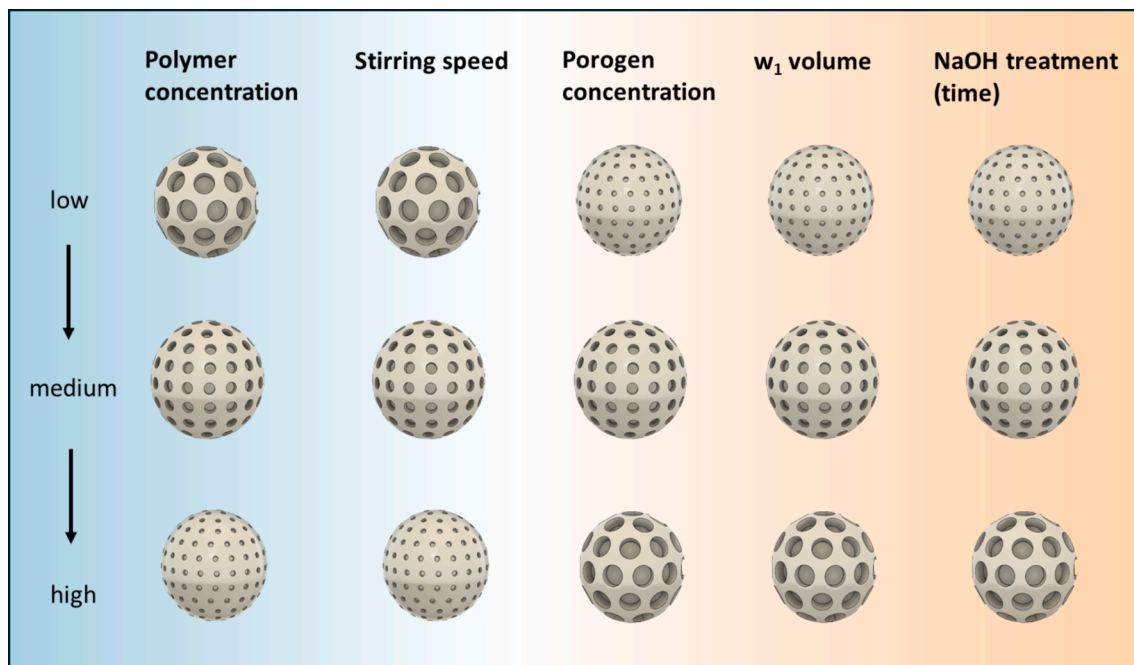


**Fig. 9.** Scheme illustrating typical effects of parameters (polymer concentration, stirring speed, porogen concentration, w<sub>1</sub> phase volume, NaOH treatment time) on the porosity and pore sizes of microparticles.

### 2.1.6. Fabrication temperature

Temperature exposure (heating, cooling) during the fabrication process affects the viscosity of the phases, diffusion coefficients, and thus also the solvent removal/polymer precipitation rates (Blasi, 2019; Park et al., 2019). Cold processing may also be relevant to retain the stability of protein drugs and other sensitive APIs during microencapsulation.

When salmon calcitonin-loaded PLGA particles were prepared by an o/w emulsion with solvent evaporation either by a rapid or a stepwise increase of the temperature from 15 to 40 °C, a process-structure relationship with a correlation based on solvent removal rates could be established: Particles with large hollow cores and thin shells resulted from rapid heating and fast removal of the o-phase solvent, while capsules with thicker porous particle walls were seen in case of stepwise heating with a quantitatively monitored slower solvent removal (Jeyanthi et al., 1996; Mehta et al., 1994). Interestingly, isothermal solvent evaporation at six different temperatures (4 – 38 °C) did not lead to visible differences in the surface porosity of PLGA particles (w/o/w) with PEG as a porogen. However, lowest burst release and highest encapsulation efficiencies were found at both 4 °C and 38 °C but not at 22 °C, indicating that internal structure and interconnectivity of pores can differ drastically. An evaporation-driven skin formation of nascent

droplets at high temperatures and a nucleation growth/spinodal decomposition-driven skin creation at low temperatures were assigned for this phenomenon, while intermediate temperatures were less suitable to build ultrastructures that retain the API (Yang et al., 2000b). Similar effects on burst release were also observed for other proteins encapsulated at low, medium, and high evaporation temperatures (Yang et al., 2000a).

Temperature can also have an effect on porogen functionality, e.g. for volatile porogens or such porogens undergoing other temperature-dependent phase changes during solvent extraction. An increase in temperature of the hardening bath of PCL particles that were prepared with camphene as porogen resulted in bigger pores, which has been assigned to differences in camphene crystallization pattern during solvent removal (Fig. 7) (Park et al., 2016).

### 2.1.7. pH-value of water phases

Different pH values of the inner water phase of w/o/w emulsion can be required when a dissolved drug is more stable in an acidic or basic environment. At the same time, protonation states of excipients/polymers may change, additives can build osmotic pressure gradients, and acid or base remaining in the final microparticle product may affect the stability of the polyester matrix. A study tested different pH values (2.2;



**Table 1**

Properties and characteristics of porous microparticles prepared by emulsion-based methods while applying variations of different process parameters.

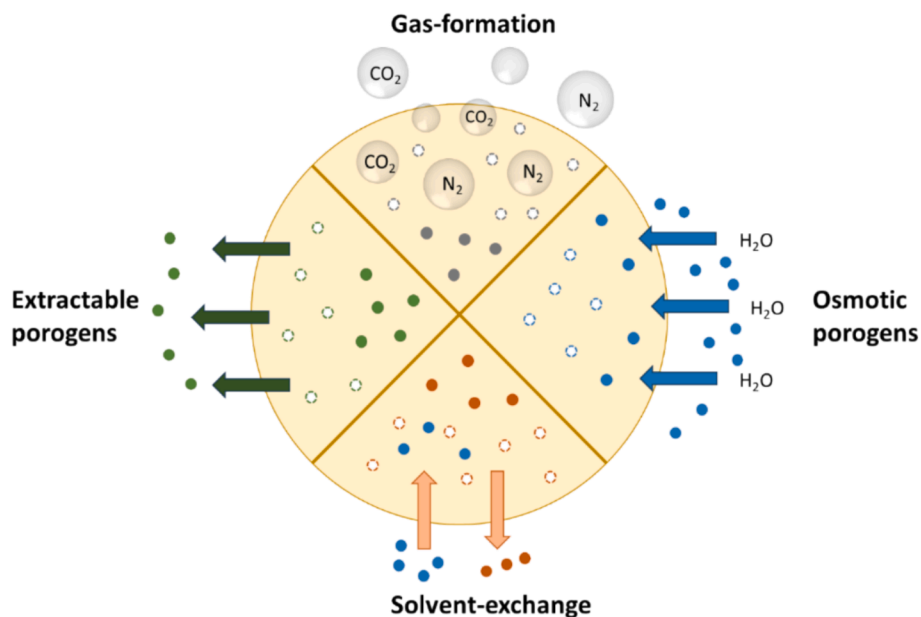
Polymer	Fabrication method	Porogen	Modified parameters	Particle sizes [ $\mu\text{m}$ ]	Porosity [%]	Pore sizes [ $\mu\text{m}$ ]	Reference
PLGA	w/o/w	n.a.	Volume of $w_1$ $\uparrow$	27 – 48	n.d.	0.22 – 1.57	(Schlicher et al., 1997)
PLGA	w/o/w	MgCO <sub>3</sub>	Volume of $w_1$ $\uparrow$	n.d.	49.5 – 64	/	(Reinhold and Schwendeman, 2013)
PLGA	o/w	Poloxamer 188	DCM/water ratio $\uparrow$	52 – 4	n.d.	0 – 5.5	(Kim et al., 2006a)
PLA	o/w	n.a.	Stirring speed $\uparrow$	471 – 176	n.d.	24 – 12	(Hong et al., 2005)
PLGA	w/o/w	ABC (15 % wt.)	Stirring speed $\uparrow$	n.d.	95 – 94.2	33 – 8	(Kim et al., 2018)
PLGA	w/o/w	ABC (1 % w/v)	PLGA conc. $\uparrow$	86 – 91	68 – 83	8 – 11	(Amoyav and Benny, 2019)
PLGA	w/o/w	n.a.	PLGA conc. $\uparrow$	27 – 88	n.d.	0.13 – 0.02	(Schlicher et al., 1997)
PLGA	w/o/w	MgCO <sub>3</sub>	PLGA conc. $\uparrow$	n.d.	61 – 72.7	/	(Reinhold and Schwendeman, 2013)
PLGA	w/o/w	ABC (1 % w/v)	PLGA conc. $\uparrow$	175.3 – 362.4	n.d.	29.4 – 7.9	(Chung et al., 2008)
PLGA	w/o/w	BSA	PLGA conc. $\uparrow$	3 – 12	n.d.	$\approx$ 0.9	(Lee et al., 2010)
PLA	o/w	n.a.	PLA conc. $\uparrow$	241 – 471	n.d.	24 – 7	(Hong et al., 2005)
PLGA	w/o/w	ABC (15 % wt.)	PLGA conc. $\uparrow$	n.d.	97.7 – 95	47.9 – 33.1	(Kim et al., 2018)
			PLGA molecular weight $\uparrow$		97.7 – 93.3	47.9 – 35.3	
PLGA 50:50	o/w	2-	PLGA molecular weight $\uparrow$	143 – 156	n.d.	3.4 – 4.4	(Zhang et al., 2014)
PLGA 65:35		Methylpentane		137 – 147		5.1 – 3.9	
PLGA 75:25				151 – 132		4.6 – 3.2	
PLA	o/w	n.a.	PVA conc. $\uparrow$	390 – 290	n.d.	10 – 16	(Hong et al., 2005)
PLGA	w/o/w	Sodium oleate	PVA conc. in $w_2$ $\uparrow$	37.16 – 4.26	n.d.	3.88 – 1.17	(Sun et al., 2009)
PLA	o/w	n.a.	Solvent/non-solvent ratio $\downarrow$	251 – 413	n.d.	5 – 30	(Hong et al., 2005)
PLGA	o/w	n.a.	Incubation time with NaOH $\uparrow$	n.d.	n.d.	7 – 22	(Lin et al., 2022)
PLGA	w/o/w	ABC (1 % w/v)	Incubation time with NaOH $\uparrow$	312 – 225	68 – 98	8 – 53	(Amoyav and Benny, 2019)
PLGA	w/o/w	n.a.	Incubation time with NaOH $\uparrow$	$\approx$ 100	n.d.	7.2 – 18.1	(Qu et al., 2021)

n.a.: not applicable.

n.d.: not determined.

ABC: ammonium bicarbonate.

BSA: bovine serum albumin

**Fig. 10.** Mechanisms of pore formation in microparticles via porogens.

3.0; 4.0; 5.0) in the inner and outer water phase of w/o/w emulsions for the fabrication of PLA particles (Herrmann and Bodmeier, 1995a). A pH value of 2.2 (adjusted with a citric acid/HCL buffer) led to highly porous particles when applied as the inner water phase. The same buffer added in both inner and outer water phases again resulted in porous particles, while buffer only in the outer water phase did not support water flux

into the particle core and thus led to particles with a dense matrix structure. These findings emphasize the osmotic effects of salts (Beig et al., 2022), buffer components, sugars or other materials as will be discussed in section 3.2.

**Table 2**  
Examples of porous microparticles prepared with gas-forming porogens.

Polymer	Fabrication method	Porogen	Modified parameters	Particle sizes [μm]	Porosity [%]	Pore sizes [μm]	Reference
PLGA	w/o/w	ABC	ABC conc. ↑	320 – 800	n.d.	1 – 40	(Lee, 2020)
PLGA	w/o/w	ABC	ABC conc. ↑	343 – 535	n.d.	10 – 20	(Kim et al., 2006b)
PLGA	w/o/w	ABC	ABC conc. ↑	6.4 – 9.2	0 – 99.6	0 – 1.5	(Oh et al., 2011)
PLGA	w/o/w	ABC	ABC conc. ↑	2.2 – 15.51	0 – 48.98	0 – 1.1	(Lazo et al., 2023)
PLGA	w/o/w	ABC	ABC conc. ↑	n.d.	8.93 – 63.4	1.45 – 2.86	(Kim et al., 2020)
PLGA	w/o/w	Sodium bicarbonate (1 %)	n.a.	34 ± 13	n.d.	7.3 ± 4.0	(Kuriakose et al., 2019)
PLA	w/o/w	H <sub>2</sub> O <sub>2</sub>	H <sub>2</sub> O <sub>2</sub> conc. ↑	5.4 – 10.8	n.d.	0.002 – 0.715	(Sharma et al., 2016)
PLGA	w/o/w	H <sub>2</sub> O <sub>2</sub>	H <sub>2</sub> O <sub>2</sub> /DCM ratio ↑	122 – 70	50 – 90	4 – 18	(Bae et al., 2009)

n.a.: not applicable.

n.d.: not determined.

ABC: ammonium bicarbonate.

DCM: dichloromethane.

### 2.1.8. Treatment of porous particles with NaOH

The post-production treatment of porous polyester particles with base can increase the porosity and pore sizes of preformed porous particles (Fig. 8), e.g. aqueous NaOH (0.1 M) (Shi et al., 2019; Yuan et al., 2018), (0.2 M) (Amoyav and Benny, 2019; Shi et al., 2009), and ethanolic NaOH solution (30 % 0.25 M NaOH; 70 % absolute ethanol) (Lin et al., 2022; Qutachi et al., 2014). The complete hydrolysis of polyester microparticles in such a diluted base may take long periods of time; still, a short incubation can be sufficient to increase the pore sizes of both smaller and larger surface pores, while inner and deeper pores seem to remain unaltered or less affected with this procedure (Qu et al., 2021; Qutachi et al., 2014). It will be necessary to evaluate on a case-to-case basis, whether the use of an ethanolic or aqueous NaOH solution is preferable for a specific microparticle product. In this decision, the solubility profiles of the API must be considered, as the drug should not be extracted during post-treatment.

### 2.1.9. General trends of pore formation in emulsion techniques

In the previous sections, several parameters with a known impact on the porosity of polyester microparticles are presented. A schematic of how these parameters may affect pore sizes in traditional emulsion-based techniques is presented in Fig. 9. Some exemplary quantitative data are compiled in Table 1. It must be emphasized that the effects presented in Fig. 9 are trends and may not be universally applicable relationships. Given the mutual impact of the here reported parameters and the potential influence of further unknown parameters (e.g. associated with the specific formulation, setup, process, or sample handling), a delicate fine-tuning of microparticle preparation processes will be required to obtain products with the desired pore sizes and overall porosity.

## 3. Porogens

Porogens, i.e. pore-forming agents, may operate through different mechanisms but eventually result in the formation of pores, as will be detailed below. Many porogens are compatible with different fabrication techniques, but traditionally they are mainly used in emulsion-based methods. There is a large variety of materials that can be used as porogens, stretching from gas-forming materials to osmotic agents (salts, sugars) and extractable components such as lipids, other oil-soluble substances, as well as polymeric materials (Lagrega et al., 2020; Lakshmi et al., 2022; Lee and Sah, 2016; Nasr et al., 2013; Wang et al., 2023b). Porogens can either be dissolved or suspended in an inner water phase ( $w_1$  in case of  $w_1/o/w_2$  emulsions) or the o-phase.

Porogens and their possible decomposition products should be inert, potentially extractable during a washing step with ideally non-toxic solvents, and should not polymerize or react in a chemical way with the matrix polymer (Mansour et al., 2020). Many different types of materials matching these requirements can be used as porogens,

ultimately operating by different principles (Fig. 10).

### 3.1. Gas-forming porogens

The most commonly used substances for the production of porous scaffolds via gas formation are water-soluble carbonate salts like ammonium bicarbonate or sodium bicarbonate (Kuriakose et al., 2019). Their ability to form highly interconnected pore systems in combination with open porous surface patterns is based on decomposition and subsequent release of volatile ammonia and carbon dioxide, respectively. Slightly acidic conditions or elevated temperatures have been used to activate the gas release and foaming in model studies (Nam et al., 2000). It is advised to have a critical judgment of the required temperatures for gas production compared to reasonable processing conditions to preserve microparticle integrity. For magnesium carbonate, the role of osmotic effects during pore creation in addition to the formation of gas bubbles (CO<sub>2</sub>) has been emphasized (Reinhold and Schwendeman, 2013). The same may be applicable to the previously mentioned salts. It was also noted that gas bubbles originating from the  $w_1$  phase of  $w_1/o/w_2$  emulsions are supportive to stabilize the primary emulsion (Kim et al., 2006b).

Another type of substance that has been used to produce porous particles by gas leaching is H<sub>2</sub>O<sub>2</sub>, which may be considered a more aggressive reagent given its oxidative effect. The formation of porous PLA or PLGA particles with aqueous H<sub>2</sub>O<sub>2</sub> solution was demonstrated (Sharma et al., 2016), and could be further enhanced by the addition of catalase in the  $w_1$  phase (Bae et al., 2009).

The production of highly porous particles with open interconnected pores is particularly interesting for pulmonary drug delivery due to a proper aerodynamic diameter as well as for in vitro or in situ tissue engineering to obtain porous particulate scaffolds for cell attachment (Emami et al., 2019; Gharse and Fiegel, 2016; Kim et al., 2006b; Mohamed and van der Walle, 2008; Yuan et al., 2018). The successful encapsulation of budesonide (Oh et al., 2011), doxorubicin (Feng et al., 2014; Kim et al., 2013; Wu et al., 2016), paclitaxel (Feng et al., 2014), artesunate (Xiong et al., 2021), oridonin (Zhu et al., 2017) and curcumin (Di Natale et al., 2020; Hu et al., 2018) in large porous microparticles for pulmonary or parenteral application has been reported. Important for these applications is the well-balanced porosity and mechanical stability of scaffolds and particles.

A tuning of porosity and pore sizes by gas foaming can be achieved by increasing the concentration of the porogen (Kang et al., 2021; Kim et al., 2020; Kim et al., 2006b; Lazo et al., 2023; Lin et al., 2022; Oh et al., 2011; Shi et al., 2018; Ungaro et al., 2010; Yang et al., 2009) or by decreasing the polymer concentration (Amoyav and Benny, 2019; Chung et al., 2008; Kim et al., 2018; Shi et al., 2009). Further information about pore sizes, porosity of particles, and employed polymers are displayed in Table 2. In case of an insufficient polymer concentration or an excessive salt concentration, the particle matrix was shown to be

**Table 3**  
Examples of porous microparticles prepared with osmotic porogens.

Polymer	Fabrication method	Porogen	Modified parameters	Particle sizes [μm]	Porosity [%]	Pore sizes [μm]	Reference
PLGA	w/o/w	MgCO <sub>3</sub> (suspended in o-phase)	MgCO <sub>3</sub> concentration ↑	n.d.	60.0 – 68.8	n.d.	(Reinhold and Schwendeman, 2013)
PLGA	w/o/w	Sodium oleate	Sodium oleate/PLGA ratio ↑	11.78 – 12.91	n.d.	1.35 – 1.53	(Sun et al., 2009)
PLGA	w/o/w	BSA	BSA/PLGA ratio ↑	11 – 12	n.d.	0.18 – 0.92	(Lee et al., 2010)
PLGA	w/o/w	BSA	BSA/PLGA ratio ↑	n.d.	n.d.	0.6 – 2.24	(Nie et al., 2015)
PLGA 50:50	w/o/w	Cyclodextrin	Cyclodextrin concentration ↑	7 – 8.8	76.66 – 81.39	n.d.	(Nasr et al., 2013)
PLGA 75:25				4.54 – 5.59	76.08 – 80.36		

*n.d.*: not determined.

*BSA*: bovine serum albumin

unstable which leads to its collapse (Shi et al., 2009). Another important aspect is that an increase in the concentration of the gas forming porogens is typically associated with an overall expansion of the particle sizes (Kim et al., 2006b; Lazo et al., 2023; Sharma et al., 2016). This is a relevant difference compared to other techniques, where nascent droplets tend to shrink during removal of the o-phase solvent. Such size alterations must be considered when selecting the emulsification technique.

### 3.2. Osmotic porogens

Osmotic porogens represent one of the most important classes of additives and are frequently used to create porous particles. This can be justified as substances like sugars or salts, which are low-cost materials available in pharmaceutical quality, have an established track record as additives e.g. as stabilizers for biopharmaceuticals or as buffer components.

Gradients of osmotic pressure created by dissolved osmotic agents inside the nascent particles cause a water influx from the continuous phase into the droplet core. In case of double or multiple emulsions, the o-phase acts similarly as a semipermeable membrane by retaining the osmotic agent in the particle while allowing water to diffuse along the osmotic gradient (Pistel and Kissel, 2000). Osmotic porogens that are suspended in the o-phase can also create osmotic pressure and thus a further water influx due to their partial solubilization in the o-phase as mediated by low amounts of water being miscible with the organic solvents (Jiang et al., 2002; Liu et al., 2021).

Obviously, the concentration of osmotic agents is a decisive factor for the obtained particle ultrastructures. Increasing concentrations of NaCl (Gupta et al., 2018; Na et al., 2012; Nasr et al., 2011; Pistel and Kissel, 2000), BSA (Lee et al., 2010; Nie et al., 2015; Ren et al., 2021), cyclodextrins (Kwona et al., 2007; Nasr et al., 2013), CaCl<sub>2</sub> (Ravivarapu et al., 2000), PBS buffer (Su et al., 2020) and sodium oleate (Sun et al., 2009) have been applied to increase porosity and pore sizes (Table 3). A comparison between different porogens (NaOH, NaCl, PBS buffer, sucrose, NaHCO<sub>3</sub>, H<sub>2</sub>O<sub>2</sub>, NH<sub>4</sub>HCO<sub>3</sub>) of similar concentrations showed that the type of porogen was more important than the concentration in order to establish a certain porosity and pore sizes in PLA microspheres (Sharma et al., 2016). The sodium and phosphate ions of PBS apparently had a strong impact on the pore formation compared to the other ions and salts (Su et al., 2020). Beside additives intentionally added as osmotic porogens, other components in the formulation of PCL or PLGA particles, namely small molecule APIs, proteins, or polypeptides such as norcantharidate (Wang and Guo, 2008a; Wang and Guo, 2008b; Wang et al., 2008), insulin (Ungaro et al., 2006), capreomycin sulfate (Giovagnoli et al., 2007), or tetracosactide (Witschi and Doelker, 1998) can also act as osmotic agents supporting pore formation.

The uptake of water-mediated by osmotic porogens can be interpreted as a swelling of the solidifying particle matrix. In case of high osmotic pressure in the w<sub>1</sub> phase, particles were reported to develop a

sponge-like morphology linked to this swelling (Ahmed and Bodmeier, 2009; Pistel and Kissel, 2000). Interestingly, swelling appears to be limited as the overall particle sizes typically remain constant even with higher concentrations of osmotic porogens (Kwona et al., 2007; Lee et al., 2010; Nasr et al., 2013; Sun et al., 2009).

If high porosity of particles should be avoided, osmotic agents may be added to the continuous water phase. Water flow that proceeds inside-out towards the continuous phase resulted in denser particles with decreased shell porosity and smooth, non-porous surfaces (Beig et al., 2022; Herrmann and Bodmeier, 1995a; Jiang et al., 2002; Luan et al., 2006; Nasr et al., 2011; Pistel and Kissel, 2000; Wang and Guo, 2008a; Zhang and Zhu, 2004). In some cases, a shrinkage of (pre-solidified) particles provided dimpled surface structures (Nasr et al., 2011).

A third variant of using osmotic porogens is to suspend them in the o-phase. This concept has been shown e.g. for sugars and magnesium salts (Reinhold and Schwendeman, 2013; Varde and Pack, 2007; Zhang and Bodmeier, 2024; Zhang et al., 2016). As mentioned above, osmotic pressure is not only present in aqueous solutions, but can also be created in organic solutions with a low water content after partial dissolution of salts. A comparison of porous PLGA particles with nanosized and micronized sucrose suspended in the o-phase has recently been shown to result in larger pore diameters, but lower porosity with bigger, micronized sugar particles (Zhang and Bodmeier, 2024). It could also be shown for three types of salt (NaCl, sodium tartrate, sodium citrate) incorporated in macroscopic PLA scaffolds that the median pore diameter increases with the particle size of salts, while the porosity of the surface membrane increases with higher salt concentration (Mikos et al., 1994).

### 3.3. Extractable porogens

This class of porogens includes materials like different oils and other lipophilic molecules as well as hydrophilic materials including macromolecules like PEG, gelatin, and alginate. Sometimes, the term “leaching” (e.g. paraffin leaching technique) is used in the scientific community for this type of methodology. Those extractable porogens serve as a temporary filler, which subsequently can be removed by exposure to a suitable solvent. While osmotic effects may be present (Schiller et al., 1988), they may not be considered as the dominating (or only) mode of action here. It is also conceivable that the osmotic effects of polymers may be too weak to generate a fast water influx as needed for osmotic pore templating. Thus, the slower process of polymer extraction into the water phase defines their pore-forming capacity.

The solubility characteristics of polyethylene glycol (PEG) in both water and common o-phase solvents allow it to be codissolved with the respective matrix polymer. This makes PEG an interesting porogen, which is long established (Jiang and Schwendeman, 2001) and continues to be a major strategy to prepare porous particles in more recent studies. For example, PEG 3350 was shown to produce porous PLGA

**Table 4**  
Examples of porous microparticles prepared with extractable porogens.

Polymer	Fabrication method	Porogen	Modified Parameters	Particle sizes [ $\mu\text{m}$ ]	Porosity [%]	Pore sizes [ $\mu\text{m}$ ]	Reference
PLGA	w/o/w	PEI	PEI conc. $\uparrow$	2.7 – 5.5	0 – 24	0 – 0.374	(Fang et al., 2014)
PLGA	o/w	Poloxamer 407	Poloxamer conc. $\uparrow$	30 – 52	n.d.	0 – 2.6	(Kim et al., 2006a)
PLGA	o/w	Poloxamer 188	n.a.	16.2 $\pm$ 2.3	n.d.	0.5 – 2.0	(Kim et al., 2011)
PLGA	o/w	PEG (3350 Da)	PEG conc. $\uparrow$	5.39 – 12.7	4.62 – 92.46	n.d.	(Sodha and Gupta, 2023)
PLGA	o/w	PEG (10 kDa)	PEG conc. $\uparrow$	9.38 – 38.9	n.d.	0 – 2.64	(M et al., 2018)
PLGA	o/w	PVP	PVP conc. $\uparrow$	5.5 – 6.6	5.9 – 43.2	n.d.	(Zhang et al., 2020c)
					(total)	0 – 6.2	
					(internal)	0 – 17.2	
					(external)		
PLGA	w/o/w	Gelatine	n.a.	19 $\pm$ 5	n.d.	2.5 $\pm$ 1.1	(Kuriakose et al., 2019)
PLGA	o/w	Alginate microspheres	n.a.	103 $\pm$ 30	n.d.	7.4 $\pm$ 4.4	(Dhamecha et al., 2020)
PLGA	w/o/w	Mustard oil	Oil amount $\uparrow$	85 – 112	n.d.	0.2 – 2.16	(Biswal et al., 2020)
PLA	o/w	Octane, Undecane, Tridecane, Pentadecane	Porogen conc. $\uparrow$	136 – 198 (average of all decanes)	n.d.	2.5 – 6.4 2.6 – 10.1 3.7 – 13.6 3.8 – 14.2	(Baek et al., 2018)
PLGA	o/w	Petroleum ether, n-Dodecane	Porogen conc. $\uparrow$	52 – 177 48 – 83	n.d.	0.21 – 5.39 2.16 – 11.06	(Wu et al., 2022)

n.a.: not applicable.

n.d.: not determined.

PEI: Polyethylene imine.

PEG: Polyethylene glycol.

PVP: Polyvinylpyrrolidone.

particles that show a correlation between particle porosity and the employed PEG concentration (Sodha and Gupta, 2023). PEG with a higher molecular weight (10 kDa), which presumably phase separates from PLGA in the solidifying polymer matrix, resulted in more porous particles with increasing pore sizes at increasing PEG concentrations (M et al., 2018). Poloxamers are another family of polymeric porogens, which were introduced in PLA matrices. Poloxamers may be extractable and/or provide domains serving as more hydrophilic diffusion pathways for the release of biopharmaceuticals (Park et al., 1992). The pore formation by extractable porogens that form distinct individual phases in the particle matrix was also shown for PLGA microparticles with incorporated smaller alginate particles. These microparticles were initially non-porous but became porous after the alginate was extracted (aided by EDTA solution) (Dhamecha et al., 2020). Similar findings were observed in several other studies, typically using warm water baths to remove the (bio)macromolecular porogens (Choi et al., 2010; Huang et al., 2012; Kuriakose et al., 2019; Lee, 2020; Ullah et al., 2017; Zhang et al., 2021). A wide variety of other polymers have been used or may be suitable as extractable porogens. Pluronic F127 (Chung et al., 2006; Kim et al., 2011; Kim et al., 2006a), Pluronic F68 (Kim et al., 2011), and polyvinylpyrrolidone (Ni et al., 2017; Zhang et al., 2020c) can be codissolved with polymers like PLGA in the o-phase and, due to their water solubility, later extracted to the continuous water phase in emulsion based particle preparations. Polyethylene imine showed concentration-dependent effects on the porosity of PLGA particles when added to the  $w_1$  (Gupta and Ahsan, 2011) or  $w_2$  phases (Fang et al., 2014) in double emulsion techniques. The washing and extraction steps must be carried out for several hours to be completed given the slow dissolution of the macromolecules and their low diffusion rates through the polymer matrix or water-filled pores (Bridson et al., 2023). The extraction process can also lead to particles with open porosity and large surface pores (Table 4).

Lipophilic molecules like different oils (mineral and corn oil (Nasr et al., 2013), silicone oil and carnoba oil (Arnold et al., 2007), mustard oil (Biswal et al., 2020), camphene (Han et al., 2022; Park et al., 2016), glycerol monooleate (Ahmed and Bodmeier, 2009), different alkanes (octane, undecane, tridecane, pentadecane) (Baek et al., 2018), 2-

methylpentane (Zhang et al., 2014), petroleum ether, *n*-dodecane and paraffine (Wu et al., 2022), as well as medium-chain triglycerides and isopropylmyristate (Janich et al., 2019) have also been used as extractable porogens. Some of the oils mentioned above resulted in golf ball-like particles with pores at the surface that are not connected with the particle core. The formed pockets at the particle surface can be explained by the strict phase separation and coalescence of oil droplets and the polymer matrix during the solvent extraction, particle hardening, and shrinking processes. Apparently, the oil droplets tend to migrate to the particle surfaces. Some other lipophilic porogens resulted in more open porous particles, but occasionally also produced irregular and less spherical particles, as is the case for glycerol monooleate (Ahmed and Bodmeier, 2009). In some cases, washing and removal steps for the residual lipophilic materials can be laborious, requiring organic extraction media like *n*-hexane or ethyl acetate, vacuum sublimation, or rotary evaporation.

### 3.4. Solvent exchange

While organic solvents diffuse from the dispersed phase to the continuous water phase and subsequently into the gas phase through evaporation, water can flow into the dispersed phase (nascent particles). This solvent exchange also takes place, when there are no additional additives (e.g. co-solvents, osmotic agents) in the dispersed phase. The rate and extent of water influx are determined by the water solubility in that organic solvent and its interaction with the polymer, as discussed in section 2.1.4., with a continuously changing ternary setting (solvent-polymer-water). The extent of water influx from the continuous into the dispersed phase, as triggered by more hydrophilic polymers, will typically affect the porosity of microparticles (Wischke and Schwendeman, 2008).

## 4. Characterization of porosity and pore sizes

In this section, we briefly summarize techniques and methods to characterize the porosity and pore sizes of macropores (> 50 nm), as these pores are the main subject of this review. For a more in-depth



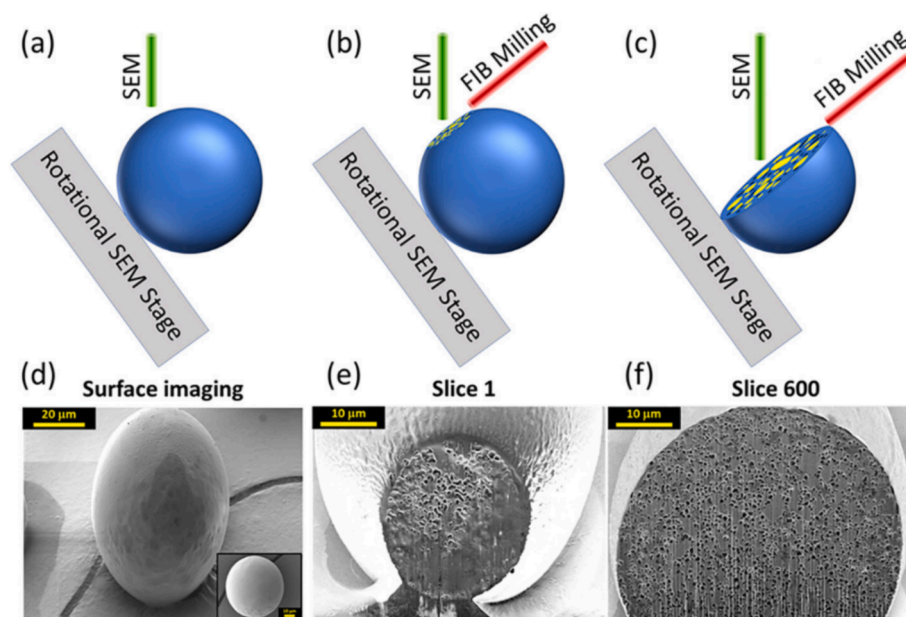


**Fig. 11.** Schematic overview of SEM imaging of PLGA microparticles on rotational SEM stage, (a) prior to FIB milling, (b) first slice and cross-sectional view, (c) 600th slice and cross-sectional view. Corresponding below are the SEM images ((d-f)). Adapted and reprinted from (Clark et al., 2022) with permission from Elsevier.

summary of these and other methods, several other detailed reviews are available (Anovitz and Cole, 2015; Bertoldi et al., 2011; Markl et al., 2018).

Analysis techniques for pores can be differentiated in methods providing quantitative data based on surfaces/volumes that are accessible from the outside of the particles during the measurement (open porous systems). Examples for these methods are, e.g., gas adsorption, mercury porosimetry, or micro-/nano- computed tomography ( $\mu$ CT, nanoCT). Additionally, qualitative methods can be used like microscopic techniques, potentially combined with sample preparation techniques such as microtomy to provide insights to inner structures of the samples. Data processing routes allow to semi-quantitatively estimate e.g. pore dimensions based on the two-dimensional information of the microscopy images. Therefore, understanding the principles of the methods is mandatory for a proper judgement of the analytical data.

**Microscopy.** Light microscopy is easy but powerful, allowing one to visualize particle size and shape without the need for complex equipment. However, in most cases, it is less suitable for detailed analysis of pores due to the limited resolution. Therefore, other microscopic techniques are preferable, in particular SEM (scanning electron microscopy). SEM provides the required resolution to capture images of the surface structure and, after a corresponding sample preparation, the cross-sectional ultrastructure (Mylonaki et al., 2018). When scanning the sample in the SEM with a focused beam of electrons, phenomena such as the scattering of these primary electrons at the material surface and the induced emission of secondary electrons from the material can account for material contrast. Depending on the SEM operating voltage and sample materials (atomic numbers), the primary electrons may penetrate up to a few micrometers into the sample surface. Energy release during the interaction of the electrons with the sample can cause thermal artifacts, such as the fusion of pores, which is why high attention must be paid to proper analysis conditions. SEM can be combined with other techniques. For example, in combination with a focused ion beam (FIB), particles can be milled to create a cross-sectional view (Clark et al., 2022; Zhang et al., 2020b) by gradual slicing steps (Fig. 11). However, this sample preparation technique is complex, costly, and not widely available, which is why cryo-ultramicrotomy is more common in preparing cross-sections. In many cases, charging of polymer surfaces may be observed in the SEM leading to a lack of contrast, which is why samples are sputter coated with a thin layer (commonly 2–20 nm) of a

conductive material e.g., gold, chrome, or iridium. Pores and structures in the microscale should remain unaffected during sputtering, at least if a sufficiently high distance of the samples from the target/plasma source is realized to minimize thermal exposure. However, gold-sputtered samples, particularly when sputter-coated with thick layers, provide surface textures by gold clusters at sizes of up to 50 nm, which should not be misinterpreted as surface textures/surface porosity of the sample. Other sputtering materials, such as platinum used for its minimized tendency of electrical charge build-up in polymers and biological samples, or iridium and chrome that are more commonly applied in electronics and for metals, may be alternatives to gold providing better image quality in case very small pores are to be analyzed by SEM.

Transmission electron microscopy (TEM) is less commonly applied for analysis of microparticles, as it requires ultra-thin samples (obtained by microtomy), involves delicate sample handling, and again involves the risk of thermal artifacts in polymeric samples by the electron beam, which may call for cryogenic techniques (Kuei et al., 2020). Examples of using TEM for particle analysis include small microparticles (1–5  $\mu$ m) (Thickett et al., 2019), while the method is more common to visualize structural details in nanoparticles (Bootdee et al., 2017; Li et al., 2019; Niu et al., 2009).

Overall, the outstanding power of microscopic methods lies in the ability to gain an overview of sample characteristics, visualizing fine details of shapes that are not accessible by other techniques, and providing visual insights into pore size distribution. Pore sizes and, depending on sample preparation, pore depths can be analyzed manually or automatically with image evaluation software (e.g. ImageJ). However, researchers should be aware that microscopy only images small amounts of samples or individual particles, which could potentially not be representative of the entire particle population.

**Gas pycnometry.** Gas pycnometry uses inert gases such as helium, nitrogen, or argon to measure volumes occupied by a certain mass of a sample. In most cases, helium is the favored gas because it diffuses into very small pores and provides reliable data for apparent density. The sample must not contain volatile substances such as residual solvents from particle preparation, as this would falsify results. This method only provides information on the apparent density and does not provide direct access to insights into pore sizes, thus may only be more relevant for routine quality control of well-established materials rather than scientific investigation of new porous carriers.

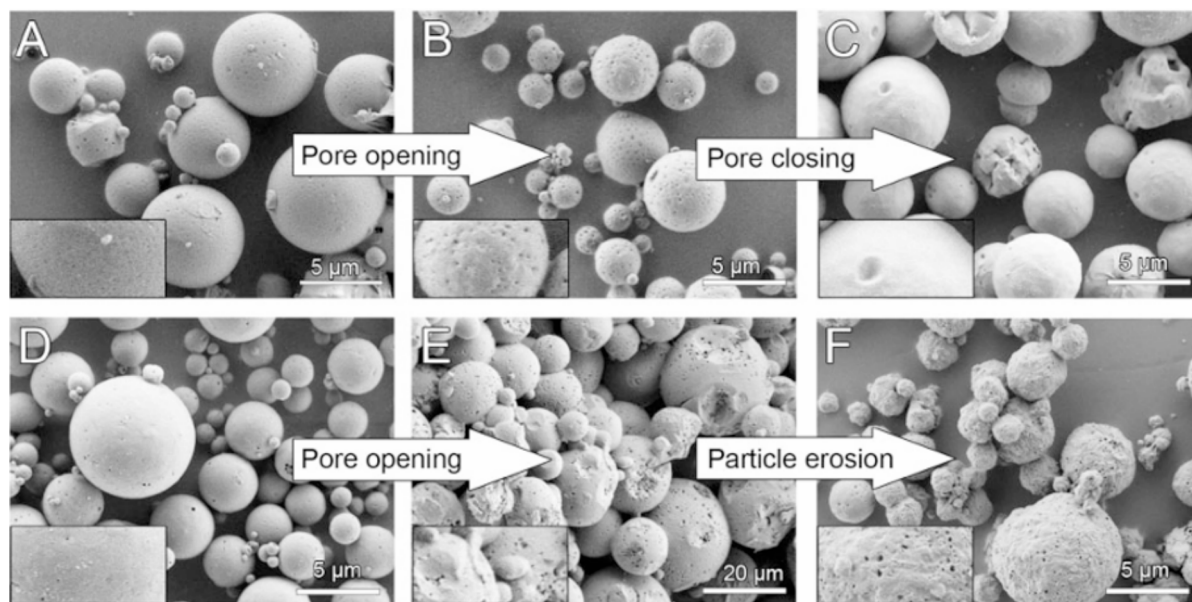


**Fig. 12.** Dynamic changes in the pore structure of microparticles from carboxyl group terminated PLGA (initial  $M_n = 5$  kDa, polydispersity 3.2) during aqueous incubation. SEM pictures A) before the incubation as well as after B) 3 h, C) 2 weeks, D) 4 weeks, E) 6 weeks, and F) 8 weeks. The insets show a detailed view at a fourfold zoom. Reprinted from (Mathew et al., 2011) with permission from Wiley.

**Gas adsorption (BET/BJH).** Gas adsorption measurements according to the BET model allow the determination of the surface areas of samples by adsorption–desorption isotherms also for such conditions, where the adsorbing gas shows a (typically undesired) multilayer adsorption. Given the small dimension of the adsorbing gas molecule, very fine pores can be reached, providing good experimental access to all open surfaces’ insight particles, as exemplified also for mesoporous PLGA nanoparticles (Tang et al., 2012). The BJH model and its recent derivatives (Yang and Wang, 2024) allow calculating pore size for micro- and mesopores, and thus may not be regularly applied for typically macroporous PLGA microparticles.

**Mercury porosimetry.** Mercury intrusion porosimetry takes benefit of the properties of mercury as a liquid metal, that is practically incompressible and non-wetting for most materials. This means that mercury will now flow into the pores by capillary forces but requires the application of increasing pressure to step-wise access finer and finer pores. According to the Washburn equation, the applied pressure during analysis is inversional proportional to the respective pore radius, while the volume of mercury taken up by the sample at a given pressure represents the overall pore volume for this specific pore size. High-pressure modules allow to analyze also very fine pores, thus making this method applicable to cover a wide range of pore diameters (5 nm – 300 µm). However, it should be noted that elemental mercury is highly toxic and poses health risks. Samples will be contaminated by this method and must be disposed of as hazardous waste. Additionally, closed pores cannot be detected. Mercury porosimetry has been applied in several studies to characterize the interparticulate and intraparticulate volumes of porous PLGA particles (Mathew et al., 2011) and has been combined in some cases with gas pycnometry, BET, and the knowledge about outer particle dimensions and size-depend powder packing densities (Vay et al., 2010).

**$\mu$ CT/nanoCT.** A non-destructive method to determine both open and closed pores is micro-computed tomography ( $\mu$ -CT).  $\mu$ CT generates volumetric and three-dimensional information about the sample by constructing a 3D model of the sample from individual 2D images obtained by X-ray scans. From this data set, multiple information such as pore volume, pore interconnectivity, specific surface area and pore surface area, and wall thicknesses can be derived. So, the advantage of this method is that the 3D data can be translated into computer models

and simulations (Pawlowski et al., 2018) and do not require a physical sectioning of a sample (Bartos et al., 2018; Menzel et al., 2023). In the biomedical field,  $\mu$ CT has been primarily used for scaffolds (Cengiz et al., 2018) or electrospun fiber meshes (Göttel et al., 2020), but can also be used to determine porous microstructures inside PLGA particles (Lefol et al., 2023). Given the limited resolution of  $\mu$ CT, often in the range of a few µm, finer details may be visible only in high-resolution nano-CT (Menzel et al., 2023). When applied to peptide-loaded PLGA microparticles, the porous network within a part of the particle could be reconstructed (Janich et al., 2019), which illustrates some limitations such as long measurement times and limited sample volume that can be reasonably depicted by nanoCT.

In addition to these established methodologies, further experimental methodologies have been applied to porous polymer particles from various materials. For instance, for particles in a liquid medium, sedimentation analysis by centrifugation was performed either in a medium with or without a density gradient material. As the particles’ pores were filled with a lower-density fluid, buoyancy resulted in a size separation of the particles and a settling velocity in a given force field depending on their porosity (Kato et al., 2022). The sedimentation of PLGA particles was also studied by flow imaging microscopy in media of different densities, where a fitting of the particle size-normalized sedimentation velocity where used to determine particle density and calculate particle porosity (Sediq et al., 2017). Such methods may need less sample quantities than some of the conventional methods, such as mercury porosimetry or gas adsorption methods. Overall, out of all of these methods, it is most common to combine SEM imaging with mercury porosimetry to characterize porous microparticles, given their suitability for the expected particle and pore size ranges.

## 5. Pore dynamics in polyester microparticles

Pore structures in polyester microparticles should not be considered as being static and unchangeable. In contrast, pores can be subject to dynamic changes that are induced by interfacial phenomena, thermal events, mass transports like water uptake, or polymer degradation. For instance, dynamic changes in the surface texture of particles can include an initial pore opening (Fig. 12).

Changes in pore structures can occur at different time scales and can

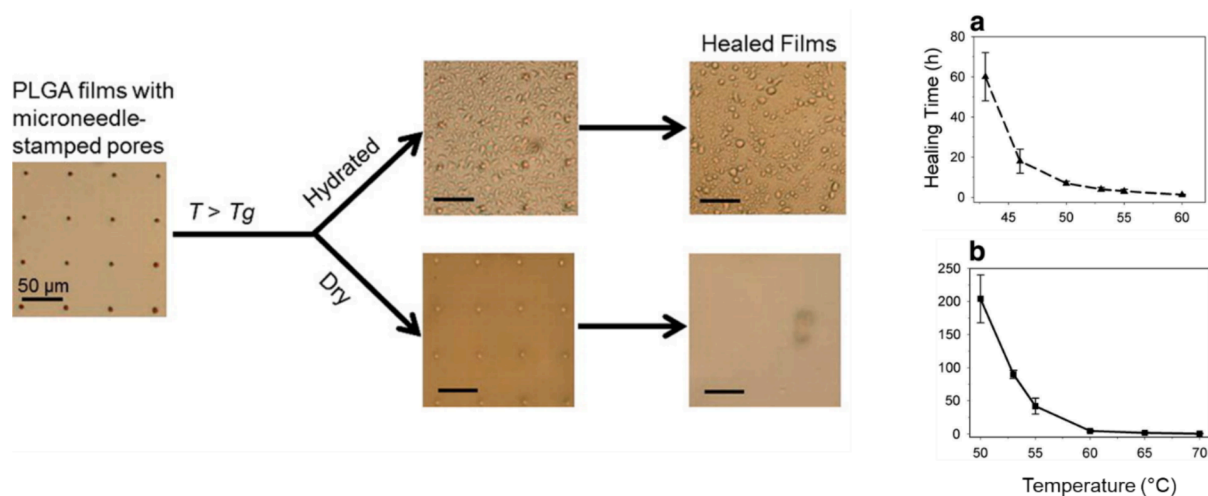


**Fig. 13.** Kinetics of pore closing depending on incubation temperature and presence/absence of water. Pores of defined sizes (5  $\mu\text{m}$ ) were introduced in PLGA films with microneedle patches. The films were incubated at elevated temperature with exposure to PBST buffer and in dry state until pore closing had been completed. Healing times depending on incubation temperatures are presented for (a) hydrated and (b) dry films. Adapted and reprinted from (Mazzara et al., 2013) with permission from Elsevier.

be driven by different mechanisms. In some studies, microparticles showed an initial opening and growth of surface pores in the first minutes to hours of incubation (Mathew et al., 2011; Wang et al., 2002). This observation can be attributed to initial drug release from the top layers of the particles and a surface rupture due to osmotic pressure created by drug molecules near the surface causing water influx (Mathew et al., 2011; Wang et al., 2002). Other mechanisms of pore growth and opening in PLGA microparticles have been linked to divalent cations (Fredenberg et al., 2007). In particular,  $\text{Zn}^{2+}$  was considered to act as a Lewis acid that catalyzes the polymer degradation, ultimately resulting in accelerated pore growth and opening.

Pore opening can be followed by a rapid pore closure during release studies in aqueous media (Fig. 12). This has notably been reported for PLGA and PLA microparticles (Mao et al., 2007; Mathew et al., 2011; Wang et al., 2002). Similar phenomena can be seen for other microstructured materials such as electrospun PLGA meshes (Khan et al., 2022; Zech et al., 2020). Obviously, the alteration of surface structures will be linked to a change in diffusion barriers and thus can affect the release profiles of encapsulated APIs including protein drugs (Kang and Schwendeman, 2007; Schutzman et al., 2023; Wang et al., 2002). Penetration assays with dye-labeled macromolecular probes, which are externally added to the suspension medium and monitored for invasion of the particles, allow determining diffusion coefficients over time and thus provide a functional in situ measure of alterations of the accessibility of porous networks in the particles (Schutzman et al., 2023).

After pore closing it is not uncommon to see further changes in particle ultrastructure. Pore opening in particles can occur as a consequence of the degradation of the polymer matrix, causing osmotic effects and a mass loss by oligomeric fragments (Fig. 12). The time frame between pore closure and pore opening depends on the degradation characteristics of the used polymer, but can also depend on the pH (Zolnik and Burgess, 2007) as well as matrix characteristics like internal porosity (Keles et al., 2015).

The principle of pore closing has been investigated in a number of systematic studies. Schwendeman and coworkers emphasized the relevance of such structural changes in the skin layer of PLGA microparticles and linked them to a potential use in self-encapsulation (see section 5.1). In their studies, they observed the formation of a nonporous skin layer via pore closing within the first 24 h of release experiments at 37  $^{\circ}\text{C}$  in acetate buffer, which was accompanied by an increase of the internal porosity of the particles (Wang et al., 2002). Also, for PLGA microparticles that initially showed pore opening, a longer incubation period

over two weeks (Mathew et al., 2011) resulted in particles with smooth surfaces and no visible pores. Other reports confirmed morphological changes of PLGA microparticles at typical temperatures of accelerated stability tests (45  $^{\circ}\text{C}$  – 70  $^{\circ}\text{C}$ ) (Zolnik et al., 2006) or at 37  $^{\circ}\text{C}$  in PBS buffer (Mao et al., 2007).

To explain pore closing, different mechanisms like the rearrangement of polymer chains (Wang et al., 2002), volume increase due to water uptake (swelling) (Scheler, 2014), polymer plasticisation (Fredenberg et al., 2011c; Mathew et al., 2011; Mohamed and van der Walle, 2008), and self-healing driven by a reduction of interfacial tension and surface curvature (Fredenberg et al., 2011c; Huang et al., 2015; Mathew et al., 2011; Mazzara et al., 2013) have been presented. In our assessment, the interplay of several phenomena can contribute to pore closing: It is well known that amorphous materials in the glassy state (like PLGA particles at temperatures below their glass transition temperature) can undergo a viscous flow, which is extremely slow and occurs on large time scales that are not practically relevant in most cases. However, upon incubation in aqueous media, the influx of water causes a plasticization of polymers like PLGA, mediating higher chain mobility at the given temperature. This phenomenon can be detected when analyzing the glass transition temperature  $T_g$ , which will shift to lower values for plasticized PLGA in aqueous environment (Blasi et al., 2005). The enhanced chain mobility will increase the propensity for viscous flow, particularly when plasticization leads to a shift of the  $T_g$  transition range towards the given sample temperature. The ability for viscous flow, however, does not yet explain the pore closing without considering the driving force to direct this flow, which is interfacial tension leading to a stress field (Mazzara et al., 2013). Accordingly, viscous flow along this field particularly at localisations with high surface curvature (which is the case particularly for small pores) will lead to a reduction of interface sizes, i.e. a smoothening of the outer particle surface. When considering PLGA plasticization and  $T_g$  reduction, it is reasonable to find an acceleration of pore closure after exposure to an aqueous medium compared to incubation in the dry state. However, in some cases during dry state storage, higher air humidity also mediated the water uptake and plasticization of PLGA particles resulting in a transition towards shallower deep pores (Bouissou et al., 2006).

When supplementing water with fully water-miscible organic solvents like ethanol (Kim et al., 2006a), acetonitrile (Kim et al., 2006a), and DMSO (Paik and Choi, 2014) or with non-water miscible ethyl acetate (Na et al., 2012; Wei et al., 2016), pore closing can be induced and/or accelerated. However, it must be considered that excessive amounts



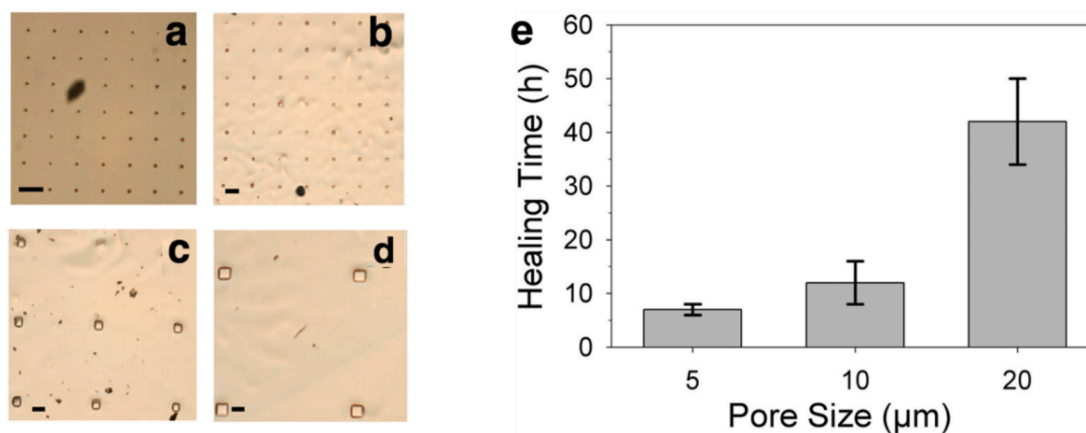


**Fig. 14.** Effect of pores sizes on healing times. Model studies with PLGA films, in which pores of a fixed depth (7 μm) and a controlled width (square-shaped cross-sectional area) were introduced with microneedle patches. Light microscopy images of pores as prepared with a) 5 μm, b) 10 μm, c) 30 μm and d) 50 μm wide (scale bar 50 μm). e) Healing time (time to full pore closing) of different pore sizes under hydrated conditions at 50 °C. Adapted and reprinted from (Mazzara et al., 2013) with permission from Elsevier.

of organic solvents result in the aggregation and fusion of microparticles (Kim et al., 2006a; Paik and Choi, 2014). Additionally, high concentrations of organic solvents could also result in a reduction of particle sizes (Kim et al., 2006a), as PLGA is partially dissolved. Organic solvents employed for pore closing could also impact the encapsulation efficiency and drug release pattern compared to pore closing without organic solvents, which will be disadvantageous and should therefore be very carefully reviewed.

It is obvious that the selected incubation temperature has a high impact on the pore closing process, with higher temperatures accelerating the rate of pore closing (Zolnik et al., 2006), while lower temperatures (below the  $T_g$  transition range) strongly reduce the rate or hinder pore closing (Fig. 13) (Mazzara et al., 2013). For instance, no change of surface morphology and internal porosity was observed for PLGA and PLGA-Glucose microparticles ( $T_g$ 's not reported) when incubated in aqueous buffer solution at 4 °C, while treatment at 37 °C resulted in a reduction of surface pores after 2 h (Kang and Schwendeman, 2007). Other reports show similar results when treating PLGA microparticles at 38 °C (Desai and Schwendeman, 2013), 42 °C (Bailey et al., 2017a), or 43 °C (Reinhold et al., 2012).

In order to describe the link between temperature and pore closing, model studies using PLGA films with highly defined pore dimensions were conducted. The Williams-Landel-Ferry Equation, which is an empirical description that is applicable to the temperature dependency of relaxation phenomena in amorphous polymers, fitted the experimental data very well and confirmed a shift towards faster pore closing kinetics if the temperature is stepwise increases above the  $T_g$  (Mazzara et al., 2013).

It should be noted that pore closing may not be observable in all cases. For example, pore closing may not be seen in polymers with high molecular weight and/or high  $T_g$  (Faisant et al., 2002; Zolnik et al., 2006), in matrices with a semi-crystalline polymer morphology that counteracts viscous flow, or when pores are relatively large. Additionally, pore formation caused by polymer degradation during longer incubation periods can counteract pore closing. For instance, a doubling of pore sizes in PLGA films has been shown to result in a drastic increase in the time needed for pore closing (Fig. 14), while in some cases pore closure was not observable when pores were too big (Mazzara et al., 2013). PLGAs with higher molecular weight showed slow or no pore closure (Fredenberg et al., 2011c; Mathew et al., 2011), e.g., no alteration of pores in films from 75:25 PLGA with ethyl end groups (80 kDa, dry state  $T_g$  50 °C) were observable while a 50:50 PLGA-COOH (12 kDa, dry state  $T_g$  42 °C) showed pore closing under various conditions. In the same study, it was shown that contact angles of hydrated PLGA films

were substantially different (28° for PLGA-COOH 12 kDa versus 49° for PLGA-Ethyl 80 kDa), indicating that higher solid/liquid interfacial free energy for PLGA-Ethyl (as the driving force for pore closing) alone is not sufficient to observe viscous flow in relevant time scales. Less plasticization of hydrophobic polymers in the presence of water as well as the entanglements of polymer chains are likely the main factors that made the hydrophobic higher molecular weight PLGA-Ethyl less efficient to close pores compared to the other polymer with lower molecular weight and better interaction with water (Fredenberg et al., 2011c). The relevance of interaction with water was also shown when introducing a 10 kDa hydrophilic PEG chain segment into PLGA (PLGA-PEG-PLGA, 70 kDa). PLGA-PEG-PLGA has a pore closing process similar to pure PLGA, which, however, occurred faster for PLGA-PEG-PLGA probably due to the lower  $T_g$  and the enhanced water uptake mediated by the hydrophilicity of the PEG domains (Mathew et al., 2011). In contrast, for 50:50 PLGA with either carboxyl (38–54 kDa;  $T_g$ , dry 45 °C,  $T_g$ , hydrated 19 °C) or lauryl ester end groups (55 kDa;  $T_g$ , dry 41 °C,  $T_g$ , hydrated 24 °C), a faster pore closing kinetic was demonstrated for PLGA-Lauryl. This observation showed that in this case, higher hydrophobicity (higher driving force) allows for pore closing to occur faster (Mazzara et al., 2013). Pore closing in polymers with very low molecular weight (e.g. 2 kDa) seems difficult to observe due to rapid polymer degradation.

Given the fact that local pH values may vary for particles in a practical setting such as by acidic additives/products or local pH shifts in the tissue, the effect of the pH-environment on the pore closing of PLGA polymers was investigated. Two competing mechanisms may be considered: accelerated degradation at low pH (Zolnik and Burgess, 2007) versus shifts in plasticization due to an altered end group-protonation and water uptake. Lower pH values (pH 3) have been shown to result in faster pore closing of 50:50 PLGA-COOH 12 kDa in comparison to neutral pH (Fredenberg et al., 2011c). Lower deprotonation of PLGA-COOH at pH 3, higher contact angles, and enhanced hydrophobic polymer-polymer interactions may have supported the more rapid minimization of the surface area in this specific case.

A comprehensive mathematical description of pore closing and changes in particle surface structures is quite challenging given the contribution of temperature, polymer properties like  $T_g$  and molecular weights (entanglements), wettability, water diffusion, plasticization, contact angles, volume changes by swelling, etc. When simplifying the problem to an amorphous polymer system that is above the glass transition temperature and is able to undergo viscous bulk flow driven by force fields at its surfaces, a mechanical model of a viscoelastic material (Maxwell model) can be applied (Huang et al., 2015). In such an approach, convex surface structures produce a compressive stress, while



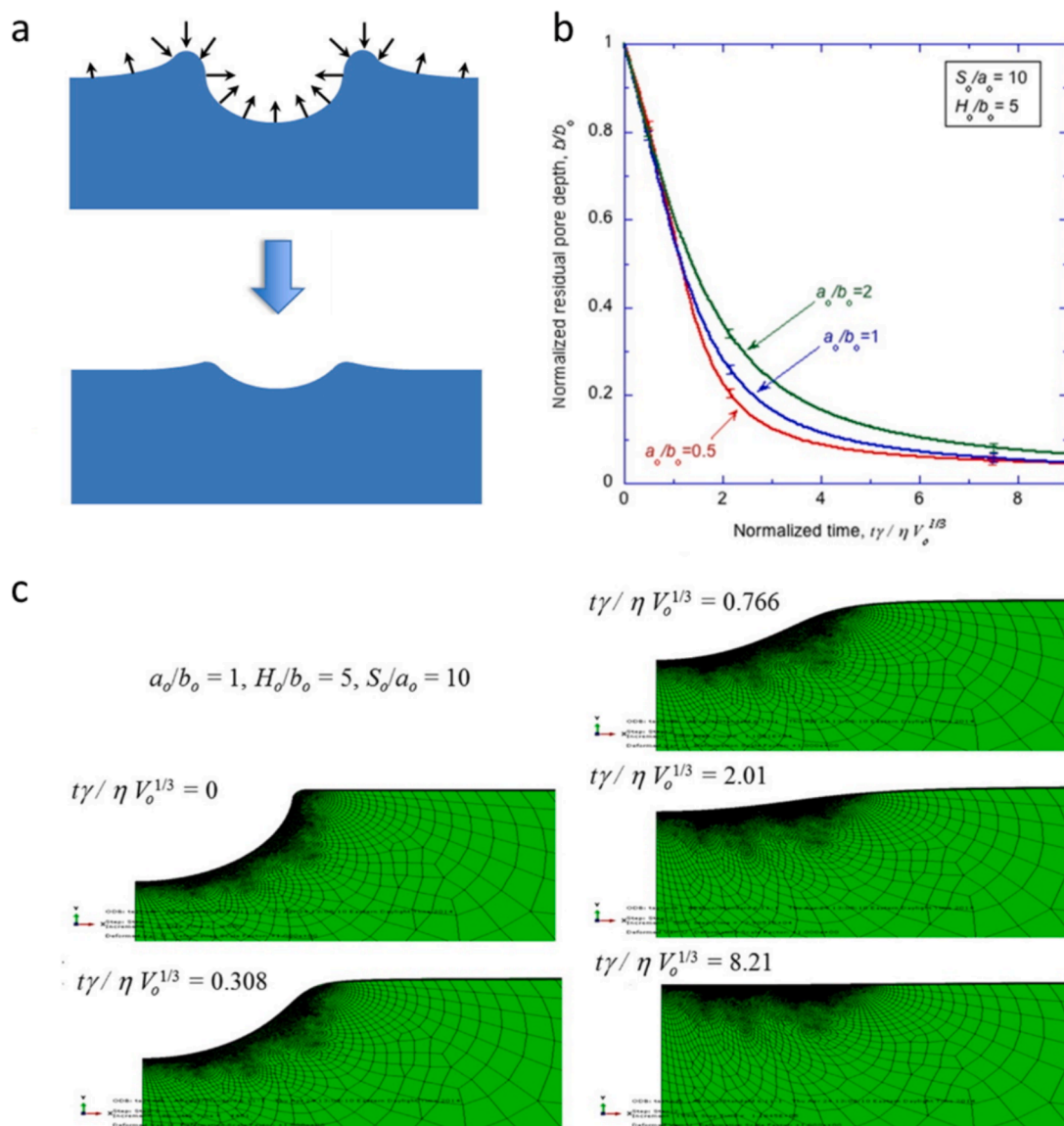


**Fig. 15.** Finite element analysis of pore closure for indents in polymer films assuming a viscoelastic Maxwell material undergoing a bulk flow based on stress fields at the material surface. (a) Schematic illustration of the healing process showing bottom-up eversion and pore size reduction driven by stress from surface curvature. The local stress fields are illustrated normal to the surface at concave and convex structures. (b) Numerical results of changes on pore depth of ellipsoidal surface pores as a function of time. In this plot, the time,  $t$ , has been normalized by the surface tension  $\gamma$ , the viscosity  $\eta$ , and the initial volume of the pore  $V_0$ . Wider and shallower pores of the same initial volume require longer times to reach the same level of healing. The error bars on these plots correspond to numerical uncertainties associated with mesh size. (c) Numerical results show how the cross-sectional profile of a surface pore  $a_0 = b_0$  (pore radius  $a_0$ , pore depth  $b_0$ ) evolves with time. Adapted and reprinted from (Huang et al., 2015) with permission from Elsevier.

concave surfaces are subject to a tensile stress, both being oriented normal to the surface (Fig. 15). When applying these stress fields, the local viscous flow of the polymer can be modeled by finite element analysis to reach endpoint conditions where an equivalence between the stresses applies. For polymer films with indents, the model shows that surface dynamics originates at the bottom of the cavities (Fig. 15). The model also indicates that healing rates decrease as the pore depth  $b_0$  for a fixed pore radius  $a_0$  decreases (Huang et al., 2015). It would be interesting to apply such models to more complex shaped porous networks with  $b_0 \gg a_0$ . This would help to understand, under which conditions a viscous flow of material at a particle surface can be achieved, resulting in a top-coverage of pores rather than their bottom-up eversion.

## 6. Pore functions in drug carriers

### 6.1. Self-encapsulation and remote-loading of drugs

Given the instability of sensitive molecules like proteins or peptides in traditional fabrication processes (organic solvents, high shear stress, heat development), alternative techniques that would allow for the incorporation of such payload after particle production are of interest. The basic principle of the self-encapsulation technology is that porous, drug-free microparticles are immersed in an aqueous solution of a drug, allowing drug diffusion into the pore volume where it either resides or from which it enters into the polymer phase depending on the physicochemical properties of the drug and polymers. Pore closing can then intentionally be induced by incubation at  $T > T_g$  (Fig. 16) (Schwendeman, 2005; Schwendeman et al., 2014). The self-encapsulation concept was shown to enable a higher stability and, in

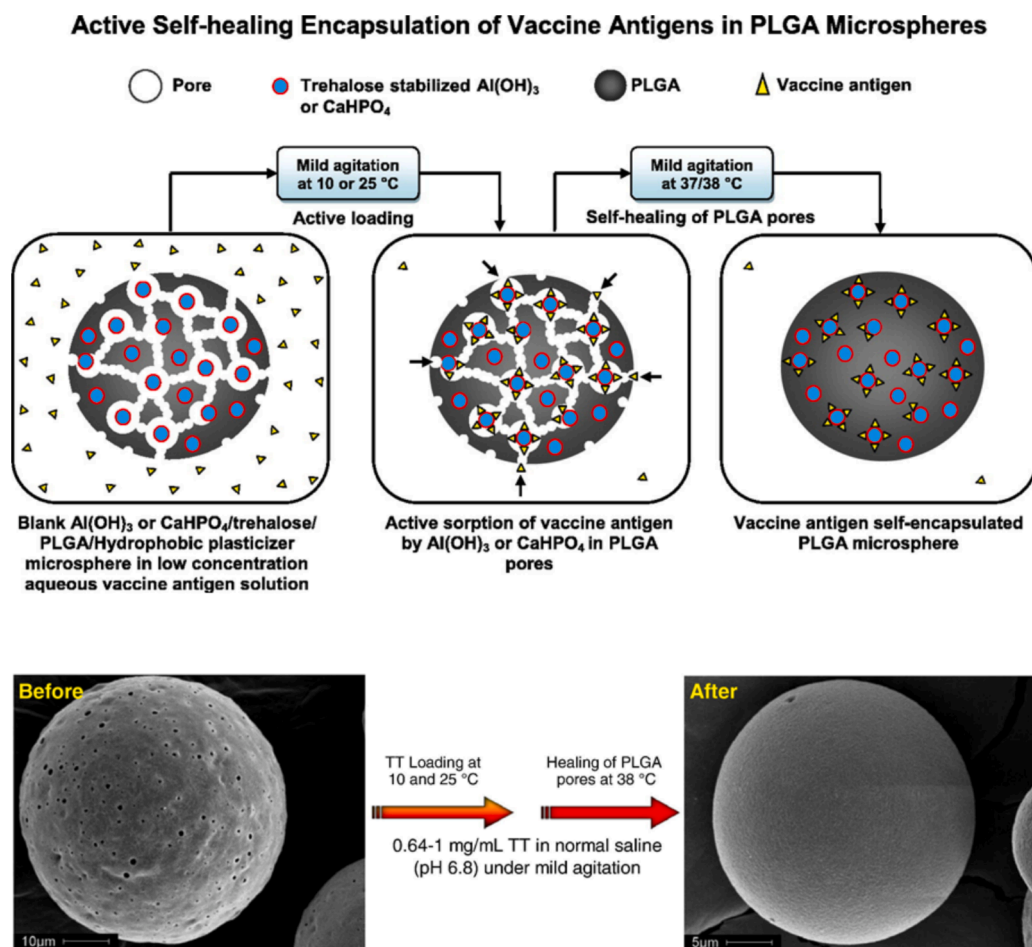


**Fig. 16.** Different stages of the self-encapsulation process. Porous microspheres (left scheme and SEM picture below) with internal protein-trapping agents (aluminum or calcium phosphate adjuvant) are mixed in an aqueous solution of antigen under mild agitation. This mixture is incubated at lower temperatures for antigen loading driven by diffusion into the pores (middle scheme). Higher temperatures above  $T_g$  are used in the last step to close the pores of PLGA and enclose the antigen (right scheme and SEM picture below). Adapted and reprinted from (Desai and Schwendeman, 2013) with permission from Elsevier.

the case of vaccine candidates, higher antigenicity compared to the classical emulsion methods (Bailey et al., 2017a; Desai and Schwendeman, 2013; Kang et al., 2021).

The porous particles, so far almost exclusively based on PLGA (Table 5), can be prepared with traditional emulsion methods using osmotic porogens like sugars (e.g. trehalose or sucrose) (Molavi et al., 2020; Yoo and Won, 2020; Zhang et al., 2020a) or any other method leading to particles with ideally small pore sizes at the surface, high porosity, and an internal interconnected pore network. Large surface pores are unfavorable as they may need too much time for pore closing or may close at all as discussed above (Mazzara et al., 2013).

One shortcoming of the self-encapsulation technology could be a restricted drug loading and loading efficiency, especially if there is no active principle allowing for accumulation of the drug in the pores. More specifically, reaching high drug loadings can be challenging as pore volumes are limited and the drug diffusion into pores is a slow and poorly controllable procedure (Kim et al., 2006a). For this reason, the use of trapping agents has been suggested, promoting to build continuous concentration gradients and thus supporting an accumulation of the drugs in the pores. For instance, Al(OH)<sub>3</sub> and CaHPO<sub>4</sub> gels incorporated into the particles could interact with (model) antigens like ovalbumin and tetanus toxoid (TT) (Bailey et al., 2017a; Desai and Schwendeman, 2013; Desai et al., 2013), while dextran sulfate was used to bind growth factors (Scheiner et al., 2021) and lysozyme (Shah and Schwendeman, 2014). Such types of bound payloads will predominantly reside in the pores once they are intentionally closed by heating during

the loading procedure.

In contrast, specific interactions between payload and polymer may mediate its entry into the polymer phase, allowing for the accessibility of a larger volume within the porous particles, larger payloads, and a prolonged release (Sophocleous et al., 2013). Peptide drugs can be particularly interesting in this context, as they may have instability issues during conventional encapsulation techniques, have been shown to well adsorb to PLGA (Calis et al., 1995), and are subject to charge interaction particularly when cationic peptides are combined with PLGA with free carboxyl end groups. Leuprolide, octreotide (Giles et al., 2022; Liang et al., 2024; Sophocleous et al., 2013), vasopressin, salmon calcitonin (Giles et al., 2022), and setmelanotide (Wang et al., 2023a) have been successfully loaded into PLGA particles by this principle, which has also been called 'remote loading' to emphasize that it works with blank porous microparticles. It was observed that the maximal sorption of peptides correlates with the number of charged carboxylic acid end groups (Sophocleous et al., 2013), which indicates an advantage of using carboxyl-terminated PLGAs for the remote loading process. Taking particle porosity as a variable parameter into account, it could be better accessibility of the polymer phase in particles with higher porosity can attain higher encapsulation efficiencies than in the case of particles with lower porosity (Wang et al., 2023a), while there were no significant differences in cumulative release observable. Pore closing, commonly an essential part of the self-encapsulation process, may not be absolutely required for the remote peptide loading strategy, but should be advantageous to establish a long-term release of the payload by a

**Table 5**

Examples of proteins and drugs encapsulated in porous PLGA microparticles via the self-encapsulation/remote-loading concept.

Polymer	Encapsulated drug	Reference
PLGA	Ovalbumin (OVA), tetanus toxoid (TT)	(Desai and Schwendeman, 2013)
PLGA	Insulin-like growth factor (IGF), vascular endothelial growth factor (VEGF), fibroblastic growth factor (FGF)	(Scheiner et al., 2021)
PLGA	Leuprolide, octreotide, vasopressin, salmon calcitonin	(Giles et al., 2022)
PLGA	Leuprolide acetate, octreotide acetate	(Liang et al., 2024)
PLGA	Setmelanotide	(Wang et al., 2023a)
PLGA	Ovalbumin (OVA)	(Bailey et al., 2017a; Bailey et al., 2017b)
PLGA	tetanus toxoid (TT)	(Desai et al., 2013)
PLGA	Antigens (rHBsAg, rPA, F1-V), Ovalbumin (OVA)	(Mazzara et al., 2019)
PLGA	Infliximab	(Hanaki et al., 2023)
PLGA	FITC-Dextran	(Paik and Choi, 2014)
PLGA/PELA blend	Ropivacain	(Wen et al., 2022)
PLGA	$\alpha$ -Amylase	(Kang et al., 2021)
PLGA	Lysozyme, FITC-Dextran	(Reinhold et al., 2012)
PLGA	BSA, lysozyme	(Reinhold and Schwendeman, 2013)
PLGA	rhGh	(Kim et al., 2006a)
PLGA	Antisense oligonucleotides	(Ahmed and Bodmeier, 2009)
PLGA	Lysozyme	(Kim and Sah, 2021)

rHBsAg: recombinant HBV surface antigen.

rPA: recombinant protective antigen.

F1-V: recombinant plague antigen.

rhGh: recombinant human growth hormone.

PELA: Monomethoxy polyethylene glycol-*b*-poly(*D,L*-lactide).

more distinct diffusion barrier. Potential limitations for this method are some restrictions in polymer type (charge, hydrophilicity, molecular weights), limitations in peptide type (charge, size/diffusivity), and potential chemical changes of peptides, e.g. acylation by polymer degradation products in the polymer phase if no additional measures are taken (Zhang and Schwendeman, 2012).

Critical process parameters for pore-closing during self-encapsulation are, e.g., temperature, incubation time, and drug concentration in the incubation solution. In addition to the most common

way of drug loading with an aqueous solution, mixtures of water with organic solvents like DMSO (up to 20 % w/w), acetonitrile (up to 20 % v/v) or ethanol (up to 40 % v/v) have been reported as loading medium. This helped to realize an accelerated pore closing also at ambient conditions, thus avoiding exposure to elevated temperatures (Kim et al., 2006a; Paik and Choi, 2014). Furthermore, the dry-state flushing of a fluidized particle bed with ethanol-saturated nitrogen was applied (Fig. 17) (Kim et al., 2006a). However, the potential effects of the organic solvents on the stability of sensitive payloads such as proteins must be investigated. Another study loaded oligonucleotides into porous microparticles and closed the surface pores with incubation at 60–80 °C

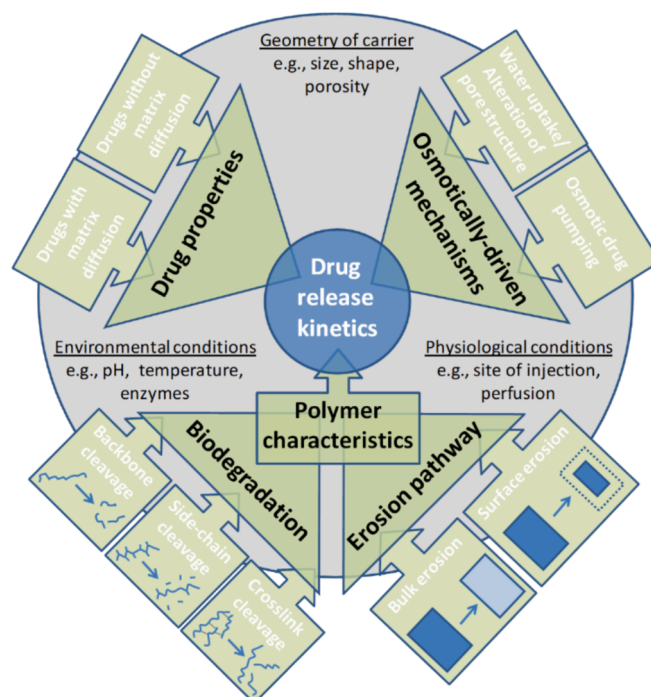


**Fig. 18.** Scheme of major factors that may influence drug release rates from drug carriers based on degradable polymers. Reprinted from (Wischke and Schwendeman, 2012) with permission from Springer Nature.

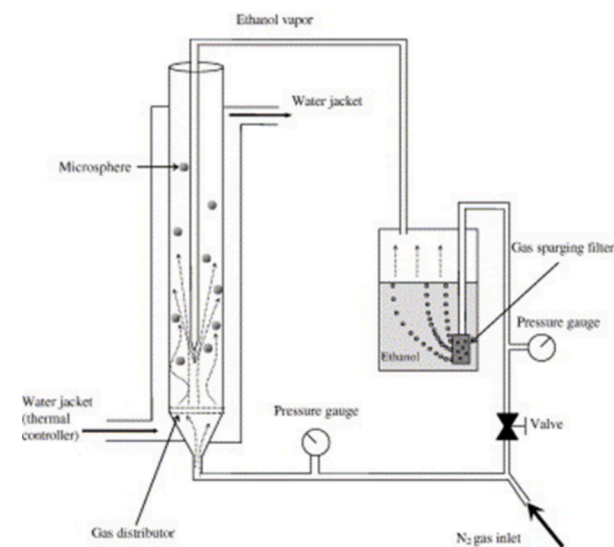


**Fig. 17.** Concept and application of ethanol vapor for pore closure of PLGA particles. (Left) Schematic diagram of the fluidized bed reactor. (Right) Surface (top) and cross-sectional (bottom) SEM pictures of PLGA particles before (left) and after (right) pore closing. Adapted and reprinted from (Kim et al., 2006a) with permission from Elsevier.



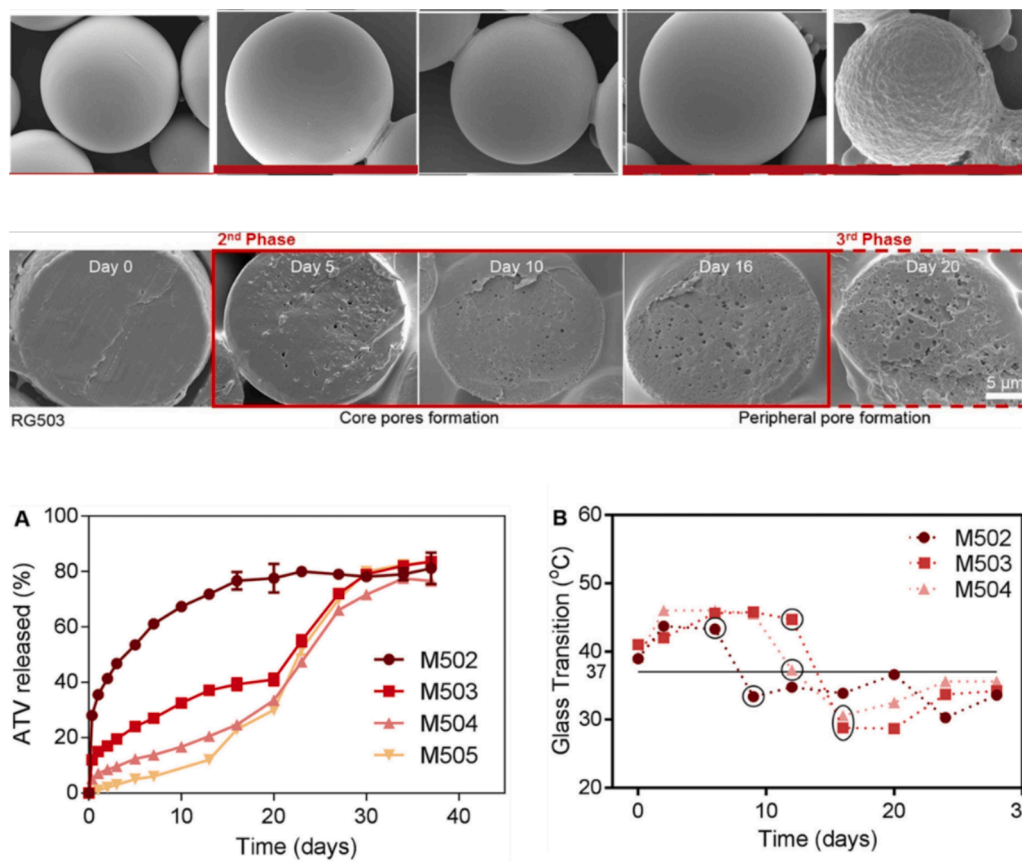


**Fig. 19.** Effect of degradation-induced changes in pore structure on atorvastatin release from PLGA microparticles made from Resomer® RG 502/503/504/505. (Top) Exemplary SEM images for RG 503 particles for 0 to 20 days of aqueous incubation. (Bottom) Quantitative analysis of (A) cumulative atorvastatin release from microparticles in vivo (0.1 M PBS pH 7.4/SDS 0.1 %) (polymers: RG 502/503/504/505) as well as (B) changes of  $T_g$  of ATV-loaded microparticles (polymers: RG 502/503/504) during the release study. Circles indicate a significant shift in the glass transition temperature. Adapted and reprinted from (Mylonaki et al., 2018) with permission from Elsevier.

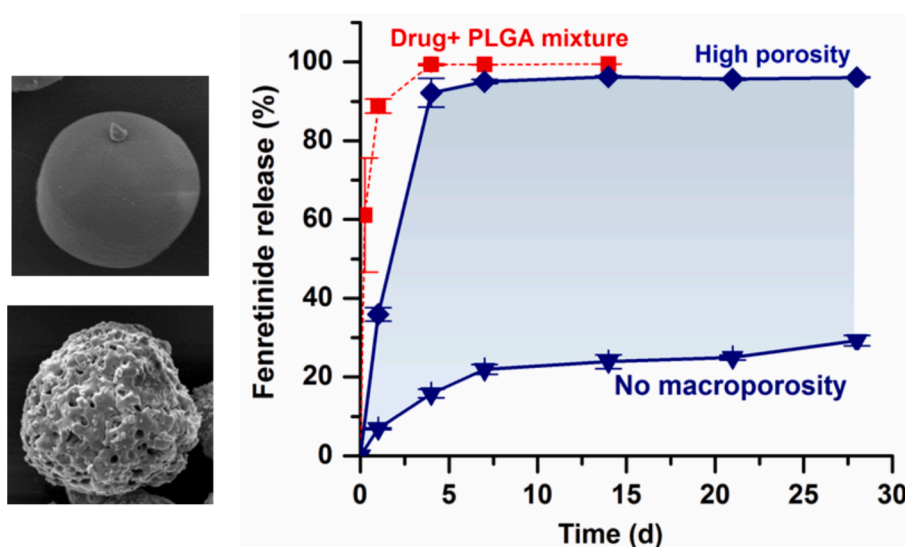


**Fig. 20.** Effect of porosity on the drug release of highly hydrophobic fenretinide from PLGA particles (Resomer® RG 503) in comparison to drug/polymer mixture. The drug release medium was 1 % (v/v) Polysorbate 80/PBS pH 7.4 at 37 °C, where the surfactant was added to enable relevant solubility. Adapted and reprinted from (Wischke and Schwendeman, 2012) with permission from Springer Nature.

in paraffin oil (Ahmed and Bodmeier, 2009). The use of plasticizers (Desai and Schwendeman, 2013), if acceptable from a toxicological point of view (note that phthalates are endocrine disruptors and should

be reduced or avoided (Arrigo et al., 2023)), may allow for reducing the  $T_g$  and thus reducing the temperatures needed for pore closing. Alternative ways of pore closing could be infrared irradiation for local



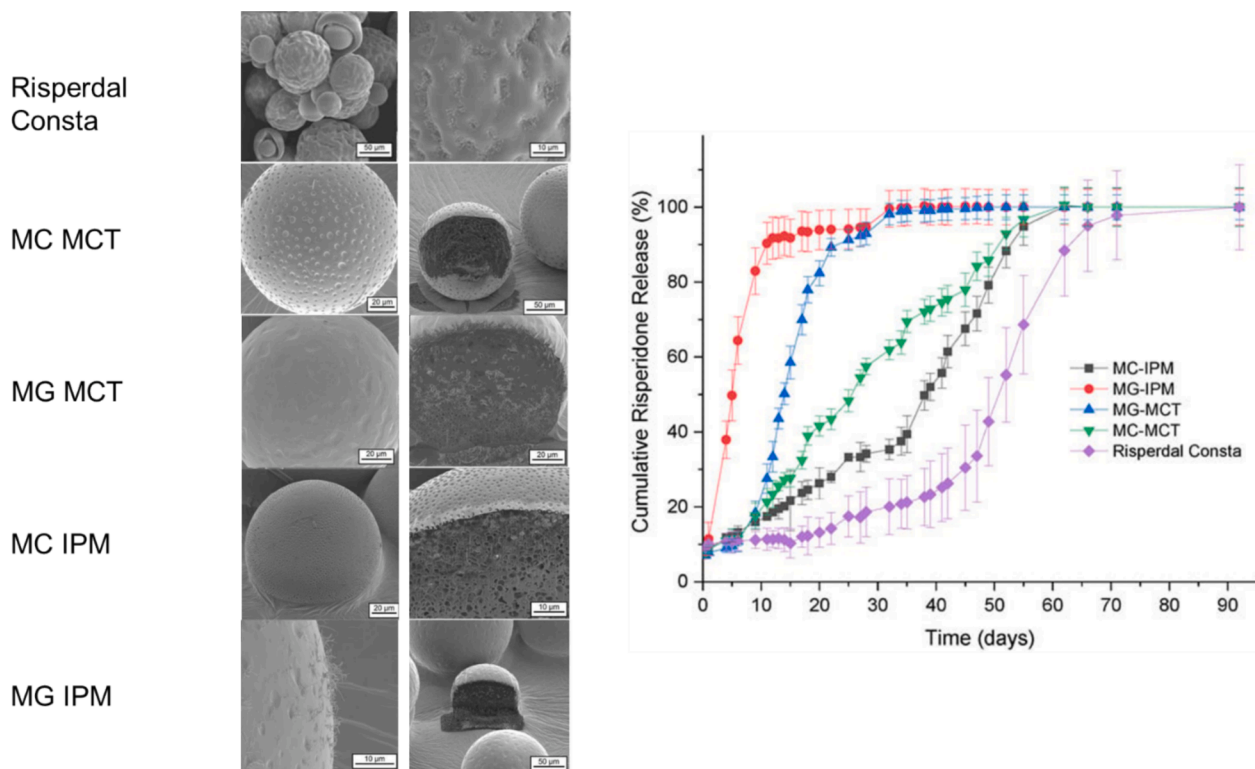


Fig. 21. Effect of porosity/lipophilic phases on the drug release of hydrophobic risperidone from PLGA particles. The particle preparation involved the addition of either isopropyl myristate (IPM) or medium chain triglycerides (MCT) to the oil phase. Particle ultrastructures were named microcapsules (MC) or microgels (MG), the latter containing an oleogelator in order to gel the IPM or MCT. (Left) SEM Images of particles. (Right) Cumulative risperidone release from the different formulations. Adapted and reprinted from (Janich et al., 2019) with permission from MDPI under a Creative Commons Attribution 4.0 International License (<https://creativecommons.org/licenses/by/4.0/>).

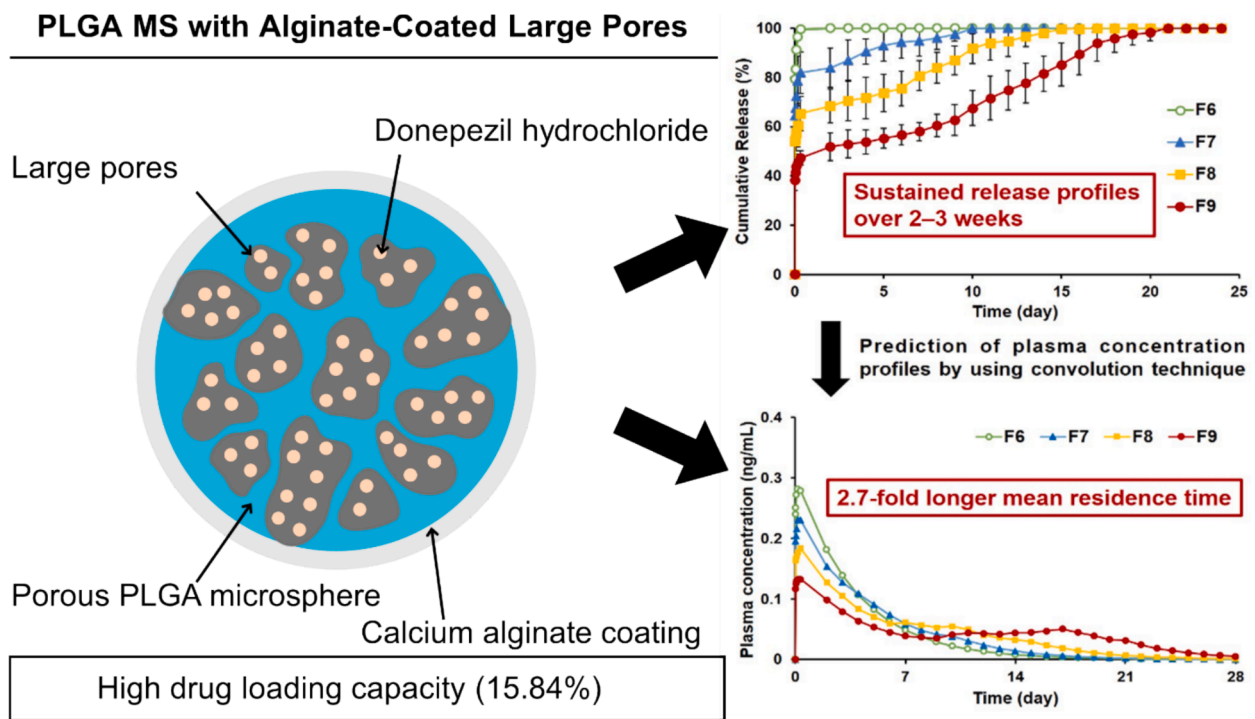
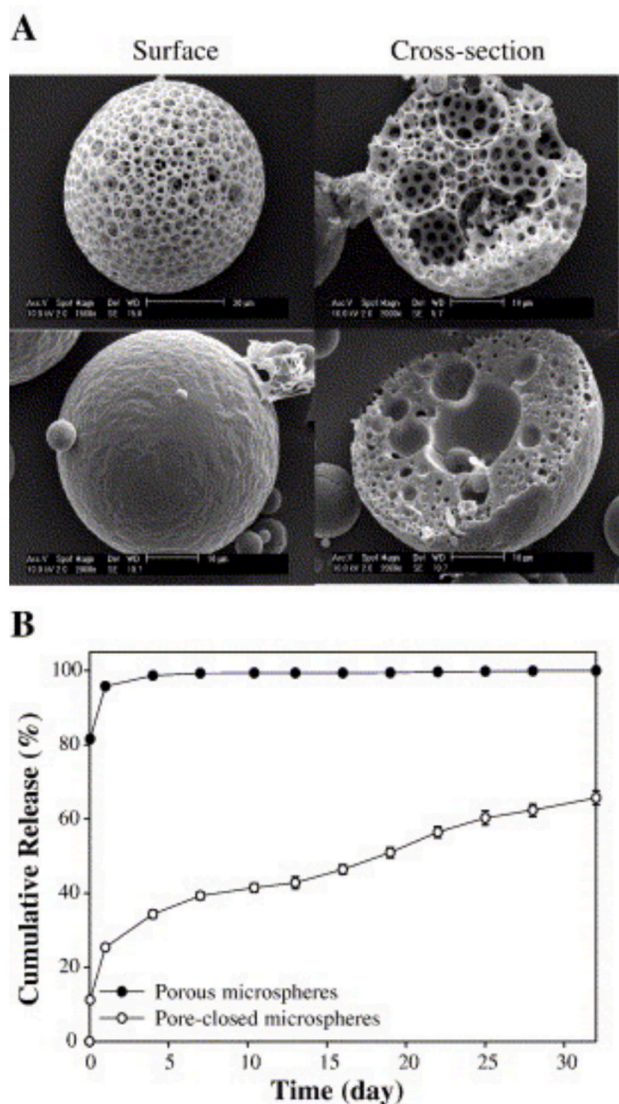


Fig. 22. PLGA microsphere with alginate-coated large pores and encapsulated donepezil hydrochloride resulting in sustained drug release of formulations (F6-F9) depending on the layer thickness of alginate coating and prediction of plasma concentrations. Adapted and reprinted from (Kim et al., 2020) with permission from MDPI under a Creative Commons Attribution 4.0 International License (<https://creativecommons.org/licenses/by/4.0/>).



**Fig. 23.** Effect of open/closed pore structure on the release of human growth hormone from PLGA microparticles. (A) SEM images of the surface (left column) and cross-section (right column) of a porous (top) and pore-closed particle (bottom). (B) In vitro release profiles. Pore-closed microspheres were prepared from pore-open particles by solvent treatment in aqueous conditions before the release experiment. Reprinted from (Kim et al., 2006a) with permission from Elsevier.

heating of the particle surfaces in the dry state (Na et al., 2012) or the coating of the loaded particles with other polymers like alginate (Kim et al., 2020; Sun et al., 2009) or silk (Wang et al., 2007).

## 6.2. Drug release

The drug release from polyester microparticles is mediated by a complex interplay of several factors depending on drug properties (e.g. solubility, molecular size), particle characteristics (e.g. porosity, drug distribution in the core), polymer characteristics (e.g. water uptake, degradation, phase separation), environmental factors (e.g. release medium, temperature), pore dynamics, and molecular changes of the drug delivery system with ongoing release time (Fig. 18) (Fredenberg et al., 2011b; Wischke and Schwendeman, 2012). In addition to diffusion that is restricted by the geometry of diffusion pathways in the (porous) particle matrix and is affected by phase distribution phenomena based on polymer-drug interaction, other mechanisms can – time-dependently – contribute to drug release from PLGA and PLA-based

delivery systems such as polymer degradation, matrix erosion, and osmotic pumping phenomena (Fredenberg et al., 2011b; Wischke and Schwendeman, 2012).

When porous polyester microparticles are incubated in aqueous media, water begins to diffuse into the pores and voids of the particles. This diffusion process is driven by osmotic pressure and concentration gradients between the external environment and the polymer matrix. Porous matrices with interconnected pores allow water to penetrate more deeply into the inside of the particle; thus, a higher amount of water will be available for drug solubilization and diffusion processes already at the beginning of the incubation (Biswal et al., 2020; Khaliq et al., 2021). As a consequence of water diffusion into pores, the hydration and potentially the swelling of the polymer phase, its plasticization, and, if applicable, the hydrolytic polymer degradation and matrix erosion may be accelerated. It could be shown that the time points of degradation-induced pore formation may depend on polymer properties like initial molecular weight and correlate with a drop in glass transition temperature of the remaining (freeze-dried) polymer matrix (Mylonaki et al., 2018). Two classes of pores may be distinguished: Bigger pores in the particle core forming first and smaller peripheral pores, which are believed to mediate a second phase of accelerated drug release (Fig. 19) (Mylonaki et al., 2018). In other cases, mixed effects of initial particle porosity, matrix polymer properties, and drug-catalyzed PLGA degradation on drug release pattern were reported (Kohno et al., 2020). Generally, the heterogeneous bulk degradation by autocatalytic effects of oligomeric degradation products is well established to occur even for small PLGA/PLA microparticles. It may be speculated that particles with higher initial porosity (macropores) would accumulate less degradation products and thereby show less contributions of autocatalysis to their structural change during release conditions. As autocatalysis also shows a positive correlation with particle size, the lack of such autocatalytic pore formation in porous compared to non-porous microparticles of different sizes can result in noticeable size effects of drug release. In porous particles, increasing the diffusion length within particles of increasing sizes (7–50  $\mu\text{m}$ ) resulted in slower drug release (Klose et al., 2006; Siepmann et al., 2005).

The presence of water-filled macropores as diffusion pathways is particularly relevant for bigger molecules like proteins or peptides, while some smaller molecules may also diffuse through the polymer phase of compact particles (Fredenberg et al., 2011b). E.g., diffusion of lysozyme was found to be significantly higher in porous PLGA films than compared to non-porous films (Fredenberg et al., 2011a). For PLGA microparticles prepared with a cyclodextrin derivate as porogen and BSA as a model protein, it could be shown that higher porosity of microparticles results in a higher initial burst and drug release overall (PM<sub>0</sub> vs. PM<sub>3</sub>) (Lee et al., 2007). However, for some small molecules, particularly those of very low water solubility, high porosity can also help to tune release rates. This can be exemplified by a salt-induced alteration of PLGA particle porosity that opened a spectrum of release rates of fentanyl, which is extremely poorly soluble in water (Fig. 20) (Zhang et al., 2016). Similarly, poorly water-soluble risperidone could be either more continuously or more rapidly released from PLGA particles when pores were introduced by the addition of lipophilic components to the polymer phase (Fig. 21) (Janich et al., 2019).

Pores as diffusion pathways may also be altered after particle production to modulate release rates. If the pores as diffusion pathways are blocked, drug release rates can be reduced. This has been illustrated for alginate surface coating (Fig. 22) (Kim et al., 2020) and temperature-induced pore closing of PLGA particles (Fig. 23) (Kang and Schwendeman, 2007; Kim et al., 2006a).

It must be emphasized that the presence/absence of pores can have strong and very characteristic effects on the overall pattern of release curves, which very often differ from an ideal zero order kinetic. Specifically, rapid early-phase drug release (burst release) and/or subsequent lag-phase of almost no release are typical points of concern of injectable sustained release formulation in general. High initial releases

may, on the one hand, be observed from very porous particles, which might be acceptable for drugs with a broad therapeutic index. On the other hand, the permanent presence of pores as diffusion pathways under release conditions may also enable shorter lag times (or even an absence of lag periods) and thus facilitate an advantageous more continuous release pattern (Amoyav and Benny, 2019; Kim et al., 2006a; Kohno et al., 2020; Mao et al., 2007).

## 7. Conclusion

The porosity of microparticles as drug carriers is a highly important characteristic affecting water uptake, drug diffusion, and particle degradation. Porous particles can be tuned in their release profiles, but can also be the basis for mild encapsulation technologies via self-encapsulation based on pore closing.

Numerous techniques to prepare such porous particles have been reported. These can be categorized by the mode-of-action of employed porogens (e.g. osmotic agents) and fine-tuned by changing process parameters e.g. in emulsion-based techniques. Importantly, as pore formation is mediated by certain combinations of parameters in a multidimensional parameter space, specific knowledge and consideration of their interplay is the key to reproducible fabricate particles with an optimal pore morphology that suits the needs for a specific drug and clinical application. When using certain porogens or certain post-treatments, it must be critically evaluated if potential effects such as substantial alterations of particle sizes, drug loss or inactivation during post-treatment, or residual additives or solvents are acceptable.

The ability of certain porous particles to encapsulate sensitive molecules and to modulate the drug release based on dynamic pore closure contributes more opportunities for the formulation development of long-acting injectables. While the authors are not aware of current clinical trials of products formulated by this strategy, the upcoming expiration of the basic patent from 2005 may be a trigger towards such developments.

Overall, this review emphasizes that the role of porosity of polyester microparticles should be more systematically considered when evaluating the properties and functions of microparticles as drug carriers.

## CRedit authorship contribution statement

**Simon Pöttgen:** Writing – review & editing, Writing – original draft, Visualization, Methodology, Investigation, Conceptualization. **Magdalena Mazurek-Budzyńska:** Writing – review & editing, Writing – original draft, Investigation. **Christian Wischke:** Writing – review & editing, Supervision, Project administration, Methodology, Investigation, Funding acquisition, Conceptualization.

## Declaration of competing interest

The authors declare the following financial interests/personal relationships which may be considered as potential competing interests: [Reports a relationship with that includes: Has patent pending to. If there are other authors, they declare that they have no known competing financial interests or personal relationships that could have appeared to influence the work reported in this paper].

## Acknowledgments

The authors acknowledge institutional funding by Martin-Luther University Halle-Wittenberg and have not received other funding for this work. The authors acknowledge proof-reading by Lorna Fortune.

## Data availability

No data was used for the research described in the article.

## References

- Ahmed, A.R., Bodmeier, R., 2009. Preparation of preformed porous PLGA microparticles and antisense oligonucleotides loading. *Eur. J. Pharm. Biopharm.* 71, 264–270.
- Amoyav, B., Benny, O., 2019. Microfluidic based fabrication and characterization of highly porous polymeric microspheres. *Polymers-Basel* 11 (3), 419.
- Anovitz, L.M., Cole, D.R., 2015. Characterization and analysis of porosity and pore structures. *Rev. Mineral. Geochem.* 80, 61–164.
- Arnold, M.M., Gonnann, E.M., Schieber, L.J., Munson, E.J., Berkland, C., 2007. NanoCipro encapsulation in monodisperse large porous PLGA microparticles. *J. Control. Release* 121, 100–109.
- Arrigo, F., Impellitteri, F., Piccione, G., Faggio, C., 2023. Phthalates and their effects on human health: Focus on erythrocytes and the reproductive system. *Comp. Biochem. Physiol. C: Toxicol. Pharmacol.* 270, 109645.
- Bae, S.E., Son, J.S., Park, K., Han, D.K., 2009. Fabrication of covered porous PLGA microspheres using hydrogen peroxide for controlled drug delivery and regenerative medicine. *J. Control. Release* 133, 37–43.
- Baek, S.W., Moon, S.-K., Kang, R.H., Ah, Y., Kim, H., Choi, S.-W., 2018. One-step fabrication of uniform biodegradable microbeads with unimodal and bimodal porous structures using spontaneous microphase separation. *Macromol. Mater. Eng.* 303, 1800139.
- Bailey, B.A., Desai, K.H., Ochyl, L.J., Ciotti, S.M., Moon, J.J., Schwendeman, S.P., 2017a. Self-encapsulating poly(lactic-co-glycolic acid) (PLGA) microspheres for intranasal vaccine delivery. *Mol. Pharm.* 14, 3228–3237.
- Bailey, B.A., Ochyl, L.J., Schwendeman, S.P., Moon, J.J., 2017b. Toward a single-dose vaccination strategy with self-encapsulating PLGA microspheres. *Adv. Healthc. Mater.* 6, 1601418.
- Bartos, M., Suchy, T., Foltán, R., 2018. Note on the use of different approaches to determine the pore sizes of tissue engineering scaffolds: what do we measure? *Biomed. Eng. Online* 17.
- Beig, A., Ackermann, R., Schutzman, R., Wang, Y., Schwendeman, S.P., 2022. Minimizing the initial burst of octreotide acetate from glucose star PLGA microspheres prepared by the solvent evaporation method. *Int. J. Pharmaceut* 624, 121842.
- Bertoldi, S., Farè, S., Tanzi, M.C., 2011. Assessment of scaffold porosity: the new route of micro-CT. *J. Appl. Biomater Biom.* 9, 165–175.
- Biswal, A.K., Hariprasad, P., Saha, S., 2020. Efficient and prolonged antibacterial activity from porous PLGA microparticles and their application in food preservation. *Mat. Sci. Eng. C-Mater* 108, 110496.
- Blakney, A.K., Simonovsky, F.I., Suydam, I.T., Ratner, B.D., Woodrow, K.A., 2016. Rapidly biodegrading PLGA-polyurethane fibers for sustained release of physicochemically diverse drugs. *ACS Biomater Sci. Eng.* 2, 1595–1607.
- Blasi, P., 2019. Poly(lactic acid)/poly(lactic-co-glycolic acid)-based microparticles: an overview. *J. Pharm. Investig.* 49, 337–346.
- Blasi, P., D'Souza, S.S., Selmin, F., DeLuca, P.P., 2005. Plasticizing effect of water on poly (lactide-co-glycolide). *J. Control. Release* 108, 1–9.
- Bootdee, K., Grady, B.P., Nithitanakul, M., 2017. Magnetite/poly(D,L-lactide-co-glycolide) and hydroxyapatite/poly(D,L-lactide-co-glycolide) prepared by w/o/w emulsion technique for drug carrier: physical characteristic of composite nanoparticles. *Colloid Polym. Sci.* 295, 2031–2040.
- Bouissou, C., Potter, U., Altroff, H., Mardon, H., van der Walle, C., 2004. Controlled release of the fibronectin central cell binding domain from polymeric microspheres. *J. Control. Release* 95, 557–566.
- Bouissou, C., Rouse, J.J., Price, R., van der Walle, C.F., 2006. The influence of surfactant on PLGA microsphere glass transition and water sorption: remodeling the surface morphology to attenuate the burst release. *Pharm Res-Dordr* 23, 1295–1305.
- Bridson, J.H., Abbel, R., Smith, D.A., Northcott, G.L., Gaw, S., 2023. Impact of accelerated weathering on the leaching kinetics of stabiliser additives from microplastics. *J. Hazard. Mater.* 459, 132303.
- Brunacci, N., Wischke, C., Naolou, T., Neffe, A.T., Lendlein, A., 2017. Influence of surfactants on decapeptide submicron particle formation. *Eur. J. Pharm. Biopharm.* 116, 61–65.
- Cai, C.F., Mao, S.R., Germershaus, O., Schaper, A., Rytting, E., Chen, D.W., Kissel, T., 2009. Influence of morphology and drug distribution on the release process of FITC-dextran-loaded microspheres prepared with different types of PLGA. *J. Microencapsul.* 26, 334–345.
- Calis, S., Jeyanthi, R., Tsai, T., Mehta, R.C., Deluca, P.P., 1995. Adsorption of salmon-calcitonin to plga microspheres. *Pharm. Res-Dordr* 12, 1072–1076.
- Cengiz, I.F., Oliveira, J.M., Reis, R.L., 2018. Micro-CT – a digital 3D microstructural voyage into scaffolds: a systematic review of the reported methods and results. *Biomater. Res.* 22, 26.
- Choi, S.W., Yeh, Y.C., Zhang, Y., Sung, H.W., Xia, Y.N., 2010. Uniform beads with controllable pore sizes for biomedical applications. *Small* 6, 1492–1498.
- Chung, H.J., Kim, H.K., Yoon, J.J., Park, T.G., 2006. Heparin immobilized porous PLGA microspheres for angiogenic growth factor delivery. *Pharm Res-Dordr* 23, 1835–1841.
- Chung, H.J., Kim, I.K., Kim, T.G., Park, T.G., 2008. Highly open porous biodegradable microcarriers: in vitro cultivation of chondrocytes for injectable delivery. *Tissue Eng. A* 14, 607–615.
- Clark, A.G., Wang, R.F., Qin, Y.R., Wang, Y., Zhu, A.D., Lomeo, J., Bao, Q.Y., Burgess, D. J., Chen, J., Qin, B., Zou, Y., Zhang, S.W., 2022. Assessing microstructural critical quality attributes in PLGA microspheres by FIB-SEM analytics. *J. Control. Release* 349, 580–591.
- Crotts, G., Park, T.G., 1995. Preparation of porous and nonporous biodegradable polymeric hollow microspheres. *J. Control. Release* 35, 91–105.



- Cui, F., Cun, D.M., Tao, A.J., Yang, M.S., Shi, K., Zhao, M., Guan, Y., 2005. Preparation and characterization of melittin-loaded poly (DL-lactic acid) or poly (DL-lactic-co-glycolic acid) microspheres made by the double emulsion method. *J. Control. Release* 107, 310–319.
- Desai, K.G., Schwendeman, S.P., 2013. Active self-healing encapsulation of vaccine antigens in PLGA microspheres. *J. Control. Release* 165, 62–74.
- Desai, K.G.H., Kadous, S., Schwendeman, S.P., 2013. Gamma irradiation of active self-healing PLGA microspheres for efficient aqueous encapsulation of vaccine antigens. *Pharm Res-Dordr* 30, 1768–1778.
- Dhamecha, D., Le, D., Movsas, R., Gonsalves, A., Menon, J.U., 2020. Porous polymeric microspheres with controllable pore diameters for tissue engineered lung tumor model development. *Front Bioeng Biotech* 8, 799.
- Di Natale, C., Onesto, V., Lagreca, E., Vecchione, R., Netti, P.A., 2020. Tunable release of curcumin with an in silico-supported approach from mixtures of highly porous PLGA microparticles. *Materials* 13 (8), 1807.
- Emami, F., Mostafavi Yazdi, S.J., Na, D.H., 2019. Poly(lactic acid)/poly(lactic-co-glycolic acid) particulate carriers for pulmonary drug delivery. *J. Pharm. Investig.* 49, 427–442.
- Espinosa, S.M., Patil, H.L., Martinez, E.S., Pimentel, R.C., Ige, P.P., 2020. Poly-ε-caprolactone (PCL), a promising polymer for pharmaceutical and biomedical applications: focus on nanomedicine in cancer. *Int. J. Polym. Mater Po* 69, 85–126.
- Faisant, N., Siepmann, J., Benoit, J.P., 2002. PLGA-based microparticles: elucidation of mechanisms and a new, simple mathematical model quantifying drug release. *Eur. J. Pharm. Sci.* 15, 355–366.
- Fan, T., Ye, W., Du, B., Zhang, Q., Gong, L., Li, J., Lin, S., Fan, Z., Liu, Q., 2019. Effect of segment structures on the hydrolytic degradation behaviors of totally degradable poly(L-lactic acid)-based copolymers. *J. Appl. Polym. Sci.* 136, 47887.
- Fang, K., Yang, F., Zhang, Q.Y., Zhang, T.Z., Gu, N., 2014. Fabrication of nonporous and porous cationic PLGA microspheres. *Mater. Lett.* 117, 86–89.
- Feng, T.S., Tian, H.Y., Xu, C.N., Lin, L., Xie, Z.G., Lam, M.H.W., Liang, H.J., Chen, X.S., 2014. Synergistic co-delivery of doxorubicin and paclitaxel by porous PLGA microspheres for pulmonary inhalation treatment. *Eur. J. Pharm. Biopharm.* 88, 1086–1093.
- Fredenberg, S., Jönsson, M., Laakso, T., Wahlgren, M., Reslow, M., Axelsson, A., 2011a. Development of mass transport resistance in poly(lactide-co-glycolide) films and particles - a mechanistic study. *Int J Pharmaceut* 409, 194–202.
- Fredenberg, S., Reslow, M., Axelsson, A., 2007. Effect of divalent cations on pore formation and degradation of Poly(D,L-lactide-co-glycolide). *Pharm. Dev. Technol.* 12, 563–572.
- Fredenberg, S., Wahlgren, M., Reslow, M., Axelsson, A., 2011b. The mechanisms of drug release in poly(lactic-co-glycolic acid)-based drug delivery systems-a review. *Int. J. Pharmaceut* 415, 34–52.
- Fredenberg, S., Wahlgren, M., Reslow, M., Axelsson, A., 2011c. Pore formation and pore closure in poly(D,L-lactide-co-glycolide) films. *J. Control. Release* 150, 142–149.
- Gaignaux, A., Réeff, J., Siepmann, F., Siepmann, J., De Vriese, C., Goole, J., Amighi, K., 2012. Development and evaluation of sustained-release clonidine-loaded PLGA microparticles. *Int. J. Pharmaceut* 437, 20–28.
- Gao, Y., Bai, Y.T., Zhao, D., Chang, M.W., Ahmad, Z., Li, J.S., 2015. Tuning microparticle porosity during single needle electrospaying synthesis via a non-solvent-based physicochemical approach. *Polymers-Basel* 7, 2701–2710.
- Gaspar, V.M., Moreira, A.F., Costa, E.C., Queiroz, J.A., Sousa, F., Pichon, C., Correi, J.J., 2015. Gas-generating TPGS-PLGA microspheres loaded with nanoparticles (NIMPS) for co-delivery of minicircle DNA and anti-tumoral drugs. *Colloid Surface B* 134, 287–294.
- Gharse, S., Fiegel, J., 2016. Large porous hollow particles: lightweight champions of pulmonary drug delivery. *Curr. Pharm. Design* 22, 2463–2469.
- Giles, M., Hong, J., Liu, Y.Y., Tang, J., Li, T.H., Beig, A., Schwendeman, A., Schwendeman, S., 2022. Efficient aqueous remote loading of peptides in poly(lactic-co-glycolic acid). *Nat. Commun.* 13, 3282.
- Giovagnoli, S., Blasi, P., Schoubben, A., Rossi, C., Ricci, M., 2007. Preparation of large porous biodegradable microspheres by using a simple double-emulsion method for capreomycin sulfate pulmonary delivery. *Int. J. Pharmaceut* 333, 103–111.
- Göttel, B., Silva, J.M.D.E., de Oliveira, C.S., Syrowatka, F., Fiorentinis, M., Viestenz, A., Viestenz, A., Mäder, K., 2020. Electrospun nanofibers - a promising solid in-situ gelling alternative for ocular drug delivery. *Eur. J. Pharm. Biopharm.* 146, 125–132.
- Gupta, M., Aina, A., Boukari, Y., Doughy, S., Morris, A., Billa, N., 2018. Effect of volume of porogens on the porosity of PLGA scaffolds in pH-controlled environment. *Pharm. Dev. Technol.* 23, 207–210.
- Gupta, V., Ahsan, F., 2011. Influence of PEI as a core modifying agent on PLGA microspheres of PGE(1), a pulmonary selective vasodilator. *Int. J. Pharm.* 413, 51–62.
- Han, F.Y., Thurecht, K.J., Whittaker, A.K., Smith, M.T., 2016. Bioerodable PLGA-based microparticles for producing sustained-release drug formulations and strategies for improving drug loading. *Front. Pharmacol.* 7, 185.
- Han, J.H., Kim, C.M., Kim, T.H., Jin, S., Kim, G.M., 2022. Development of in situ microfluidic system for preparation of controlled porous microsphere for tissue engineering. *Pharmaceutics* 14 (11), 2345.
- Hanaki, A., Ogawa, K., Tagami, T., Ozeki, T., 2023. Fabrication and characterization of antibody-loaded cationic porous PLGA microparticles for sustained antibody release. *AAPS J.* 25, 92.
- Herrmann, J., Bodmeier, R., 1995a. The effect of particle microstructure on the somatostatin release from poly(lactide) microspheres prepared by a W/O/W solvent evaporation method. *J. Control. Release* 36, 63–71.
- Herrmann, J., Bodmeier, R., 1995b. Somatostatin containing biodegradable microspheres prepared by a modified solvent evaporation method based on W/O/W-multiple emulsions. *Int. J. Pharmaceut* 126, 129–138.
- Hong, Y., Gao, C.Y., Shi, Y.C., Shen, J.C., 2005. Preparation of porous polylactide microspheres by emulsion-solvent evaporation based on solution induced phase separation. *Polym. Advan. Technol.* 16, 622–627.
- Hu, Y.Z., Li, M., Zhang, M.M., Jin, Y.G., 2018. Inhalation treatment of idiopathic pulmonary fibrosis with curcumin large porous microparticles. *Int J Pharmaceut* 551, 212–222.
- Huang, C.C., Wei, H.J., Yeh, Y.C., Wang, J.J., Lin, W.W., Lee, T.Y., Hwang, S.M., Choi, S. W., Xia, Y.N., Chang, Y., Sung, H.W., 2012. Injectable PLGA porous beads cellularized by hAFSCs for cellular cardiomyoplasty. *Biomaterials* 33, 4069–4077.
- Huang, J., Mazzara, J.M., Schwendeman, S.P., Thoulless, M.D., 2015. Self-healing of pores in PLGAs. *J. Control. Release* 206, 20–29.
- Jallil, R., Nixon, J.R., 1990. Microencapsulation using poly(DL-lactic acid) .3. Effect of polymer molecular-weight on the release kinetics. *J. Microencapsul.* 7, 357–374.
- Janich, C., Friedmann, A., Martins de Souza, E.S.J., Santos de Oliveira, C., Souza, L.E., Rujescu, D., Hildebrandt, C., Beck-Broichsitter, M., Schmelzer, C.E.H., Mader, K., 2019. Risperidone-Loaded PLGA-lipid particles with improved release kinetics: manufacturing and detailed characterization by electron microscopy and nano-CT. *Pharmaceutics* 11 (12), 665.
- Jeyanthi, R., Thanoo, B.C., Metha, R.C., DeLuca, P.P., 1996. Effect of solvent removal technique on the matrix characteristics of polylactide/glycolide microspheres for peptide delivery. *J. Control. Release* 38, 235–244.
- Jiang, G., Thanoo, B.C., DeLuca, P.P., 2002. Effect of osmotic pressure in the solvent extraction phase on BSA release profile from PLGA microspheres. *Pharm. Dev. Technol.* 7, 391–399.
- Jiang, W.L., Schwendeman, S.P., 2001. Stabilization and controlled release of bovine serum albumin encapsulated in poly(D, L-lactide) and poly(ethylene glycol) microsphere blends. *Pharm Res-Dordr* 18, 878–885.
- Kang, J., Cai, Y.P., Wu, Z.W., Wang, S.Y., Yuan, W.E., 2021. Self-encapsulation of biomacromolecule drugs in porous microcaffolds with aqueous two-phase systems. *Pharmaceutics* 13, 426.
- Kang, J.C., Schwendeman, S.P., 2007. Pore closing and opening in biodegradable polymers and their effect on the controlled release of proteins. *Mol. Pharmaceut* 4, 104–118.
- Kato, Y., Morimoto, T., Kobashi, K., Yamaguchi, T., Mori, T., Sugino, T., Okazaki, T., 2022. Porosity and size analysis of porous microparticles by centrifugal sedimentation with and without density gradient. *Powder Technol.* 407.
- Kazazi-Hyseni, F., Landin, M., Lathuile, A., Veldhuis, G.J., Rahimian, S., Hennink, W.E., Kok, R.J., van Nostrum, C.F., 2014. Computer modeling assisted design of monodisperse PLGA microspheres with controlled porosity affords zero order release of an encapsulated macromolecule for 3 months. *Pharm Res-Dordr* 31, 2844–2856.
- Keles, H., Naylor, A., Clegg, F., Sammon, C., 2015. Investigation of factors influencing the hydrolytic degradation of single PLGA microparticles. *Polym Degrad Stabil* 119, 228–241.
- Khalifi, N.U., Chobisa, D., Richard, C.A., Swinney, M.R., Yeo, Y., 2021. Engineering microenvironment of biodegradable polyester systems for drug stability and release control. *Ther. Deliv.* 12, 37–54.
- Khan, A., Hadano, Y., Takehara, H., Ichiki, T., 2022. Effects of physico-chemical treatments on PLGA 50:50 electrospun nanofibers. *Polymer* 261, 125400.
- Kim, D., Han, T.H., Hong, S.C., Park, S.J., Lee, Y.H., Kim, H., Park, M., Lee, J., 2020. PLGA microspheres with alginate-coated large pores for the formulation of an injectable depot of donepezil hydrochloride. *Pharmaceutics* 12 (4), 311.
- Kim, H., Kim, B.R., Shin, Y.J., Cho, S., Lee, J., 2018. Controlled formation of polylysinated inner pores in injectable microspheres of low molecular weight poly (lactide-co-glycolide) designed for efficient loading of therapeutic cells. *Artif Cell Nanomed. B* 46, S233–S246.
- Kim, H., Park, H., Lee, J., Kim, T.H., Lee, E.S., Oh, K.T., Lee, K.C., Yoon, Y.S., 2011. Highly porous large poly(lactic-co-glycolic acid) microspheres adsorbed with palmitoyl-acylated exendin-4 as a long-acting inhalation system for treating diabetes. *Biomaterials* 32, 1685–1693.
- Kim, H.K., Chung, H.J., Park, T.G., 2006a. Biodegradable polymeric microspheres with “open/closed” pores for sustained release of human growth hormone. *J. Control. Release* 112, 167–174.
- Kim, I., Byeon, H.J., Kim, T.H., Lee, E.S., Oh, K.T., Shin, B.S., Lee, K.C., Yoon, Y.S., 2013. Doxorubicin-loaded porous PLGA microparticles with surface attached TRAIL for the inhalation treatment of metastatic lung cancer. *Biomaterials* 34, 6444–6453.
- Kim, S., Sah, H., 2019. Merits of sponge-like PLGA microspheres as long-acting injectables of hydrophobic drug. *J. Biomat. Sci-Polym E* 30, 1725–1743.
- Kim, T.K., Yoon, J.J., Lee, D.S., Park, T.G., 2006b. Gas foamed open porous biodegradable polymeric microspheres. *Biomaterials* 27, 152–159.
- Kim, Y., Sah, H., 2021. Protein loading into spongelike PLGA microspheres. *Pharmaceutics* 13, 137.
- Klose, D., Siepmann, F., Elkharraz, K., Krenzlin, S., Siepmann, J., 2006. How porosity and size affect the drug release mechanisms from PLGA-based microparticles. *Int. J. Pharmaceut* 314, 198–206.
- Kohno, M., Andhariya, J.V., Wan, B., Bao, Q., Rothstein, S., Hezel, M., Wang, Y., Burgess, D.J., 2020. The effect of PLGA molecular weight differences on risperidone release from microspheres. *Int. J. Pharm.* 582, 119339.
- Kuei, B., Aplan, M.P., Litofsky, J.H., Gomez, E.D., 2020. New opportunities in transmission electron microscopy of polymers. *Mat. Sci. Eng. R* 139.
- Kuriakose, A.E., Hu, W.J., Nguyen, K.T., Menon, J.U., 2019. Scaffold-based lung tumor culture on porous PLGA microcapsule substrates. *PLoS One* 14 (5), e0217640.
- Kwona, M.J., Baea, J.H., Kima, J.J., Nab, K., Lee, E.S., 2007. Long acting porous microcapsule for pulmonary protein delivery. *Int. J. Pharmaceut* 333, 5–9.
- Lagreca, E., Onesto, V., Di Natale, C., La Manna, S., Netti, P.A., Vecchione, R., 2020. Recent advances in the formulation of PLGA microparticles for controlled drug delivery. *Prog. Biomater.* 9, 153–174.



- Lakshmi, D.S., Radha, K.S., Castro-Muñoz, R., Tanczyk, M., 2022. Emerging trends in porogens toward material fabrication: recent progresses and challenges. *Polymers-Basel* 14 (23), 5209.
- Lazo, R.E.L., Oliveira, B.D., Cobre, A.D., Ferreira, L.M., Felipe, K.B., de Oliveira, P.R., Murakami, F.S., 2023. Engineering porous PLGA microparticles for pulmonary delivery of sildenafil citrate. *Powder Technol.* 430, 118999.
- Lee, D.-H., 2020. Fabrication of biodegradable polymeric microspheres with controllable porous structure for cell delivery. *Biomedical J. Scientific & Technical Res.* 26 (BJSTR. MS.ID.004429).
- Lee, E.S., Kwon, M.J., Na, K., Bae, J.H., 2007. Protein release behavior from porous microparticle with lysozyme/hyaluronate ionic complex. *Colloids Surf. B Biointerfaces* 55, 125–130.
- Lee, J., Oh, Y.J., Lee, S.K., Lee, K.Y., 2010. Facile control of porous structures of polymer microspheres using an osmotic agent for pulmonary delivery. *J. Control. Release* 146, 61–67.
- Lee, Y., Sah, H., 2016. Simple emulsion technique as an innovative template for preparation of porous, spongelike poly(lactide-co-glycolide) microspheres with pore-controlling capability. *J. Mater. Sci.* 51, 6257–6274.
- Lefol, L.A., Bawuah, P., Zeitler, J.A., Verin, J., Danede, F., Willart, J.F., Siepmann, F., Siepmann, J., 2023. Drug release from PLGA microparticles can be slowed down by a surrounding hydrogel. *Int. J. Pharm-X* 6.
- Li, F., Wen, Y.Q., Zhang, Y., Zheng, K.Y., Ban, J.F., Xie, Q.C., Wen, Y.F., Liu, Q., Chen, F. H., Mo, Z.J., Liu, L.Z., Chen, Y.Z., Lu, Z.F., 2019. Characterisation of 2-HP- $\beta$ -cyclodextrin-PLGA nanoparticle complexes for potential use as ocular drug delivery vehicles. *Artif. Cell Nanomed B* 47, 4097–4108.
- Li, J., Rothstein, S.N., Little, S.R., Edenborn, H.M., Meyer, T.Y., 2012. The effect of monomer order on the hydrolysis of biodegradable poly(lactic-co-glycolic acid) repeating sequence copolymers. *J. Am. Chem. Soc.* 134, 16352–16359.
- Li, J., Stayshich, R.M., Meyer, T.Y., 2011. Exploiting sequence to control the hydrolysis behavior of biodegradable PLGA copolymers. *J. Am. Chem. Soc.* 133, 6910–6913.
- Liang, D.S., Frank, S., Schwendeman, S.P., 2024. Aqueous remote loading of model cationic peptides in uncapped poly(lactide-co-glycolide) microspheres for long-term controlled release. *Drug Deliv. Transl. Res.* 14, 696–704.
- Lin, A.Q., Liu, S.Y., Xiao, L., Fu, Y.Y., Liu, C.S., Li, Y.L., 2022. Controllable preparation of bioactive open porous microspheres for tissue engineering. *J. Mater. Chem. B* 10, 6464–6471.
- Liu, C.J., Dong, G.Y., Tsuru, T., Matsuyama, H., 2021. Organic solvent reverse osmosis membranes for organic liquid mixture separation: a review. *J. Membrane Sci.* 620, 118882.
- Liu, R., Huang, S.S., Wan, Y.H., Ma, G.H., Su, Z.G., 2006. Preparation of insulin-loaded PLA/PLGA microcapsules by a novel membrane emulsification method and its release in vitro. *Colloid Surface B* 51, 30–38.
- Luan, X., Skupin, M., Siepmann, J., Bodmeier, R., 2006. Key parameters affecting the initial release (burst) and encapsulation efficiency of peptide-containing poly(lactide-co-glycolide) microparticles. *Int. J. Pharm.* 324, 168–175.
- Odonchimeg, M., Kim, S.C., Shim, Y.K., Lee, W.K., 2018. Preparation of “Open/closed” pores of PLGA-microsphere for controlled release of protein drug. *Mongolian J. Chem.* 18, 41–47.
- Mansour, F.R., Waheed, S., Paull, B., Maya, F., 2020. Porogens and porogen selection in the preparation of porous polymer monoliths. *J. Sep. Sci.* 43, 56–69.
- Mao, S.R., Xu, J., Cai, C.F., Germershaus, O., Schaper, A., Kissel, T., 2007. Effect of WOW process parameters on morphology and burst release of FITC-dextran loaded PLGA microspheres. *Int. J. Pharmaceut* 334, 137–148.
- Markl, D., Strobel, A., Schlossnikl, R., Botker, J., Bawuah, P., Ridgway, C., Rantanen, J., Rades, T., Gane, P., Peiponen, K.E., Zeitler, J.A., 2018. Characterisation of pore structures of pharmaceutical tablets: a review. *Int. J. Pharmaceut* 538, 188–214.
- Mathew, S., Baudis, S., Neffe, A.T., Behl, M., Wischke, C., Lendlein, A., 2015. Effect of diisocyanate linkers on the degradation characteristics of copolyester urethanes as potential drug carrier matrices. *Eur. J. Pharm. Biopharm.* 95, 18–26.
- Mathew, S., Lendlein, A., Wischke, C., 2011. Degradation behavior of porous copolyester microparticles in the light of dynamic changes in their morphology. *Macromol. Symp.* 309–310, 123–133.
- Mazzara, J.M., Balagna, M.A., Thouless, M.D., Schwendeman, S.P., 2013. Healing kinetics of microneedle-formed pores in PLGA films. *J. Control. Release* 171, 172–177.
- Mazzara, J.M., Ochyl, L.J., Hong, J.K.Y., Moon, J.J., Prausnitz, M.R., Schwendeman, S.P., 2019. Self-healing encapsulation and controlled release of vaccine antigens from PLGA microparticles delivered by microneedle patches. *Bioeng. Transl. Med.* 4, 116–128.
- Mehta, R.C., Jeyanthi, R., Calis, S., Thanoo, B.C., Burton, K.W., Deluca, P.P., 1994. Biodegradable microspheres as depot system for parenteral delivery of peptide drugs. *J. Control. Release* 29, 375–384.
- Menzel, M., Kiesow, A., Silva, J.M.D.E., 2023. Nano-CT characterization of dental tubule occlusion in SDF-treated dentin. *Sci. Rep-Uk* 13.
- Mikos, A.G., Thorsen, A.J., Czerwonka, L.A., Bao, Y., Langer, R., Winslow, D.N., Vacanti, J.P., 1994. Preparation and Characterization of poly(L-lactic acid) foams. *Polymer* 35, 1068–1077.
- Moghanizadeh-Ashkezari, M., Shokrollahi, P., Zandi, M., Shokrollahi, F., 2018. Polyurethanes with separately tunable biodegradation behavior and mechanical properties for tissue engineering. *Polym. Advan. Technol.* 29, 528–540.
- Mohamed, F., van der Walle, C.F., 2008. Engineering biodegradable polyester particles with specific drug targeting and drug release properties. *J. Pharm Sci-U.S.* 97, 71–87.
- Molavi, F., Barzegar-Jalali, M., Hamishehkar, H., 2020. Polyester based polymeric nano and microparticles for pharmaceutical purposes: a review on formulation approaches. *J. Control. Release* 320, 265–282.
- Mylonaki, I., Allémann, E., Delie, F., Jordan, O., 2018. Imaging the porous structure in the core of degrading PLGA microparticles: the effect of molecular weight. *J. Control. Release* 286, 231–239.
- Na, X.M., Gao, F., Zhang, L.Y., Su, Z.G., Ma, G.H., 2012. Biodegradable microcapsules prepared by self-healing of porous microspheres. *ACS Macro Lett.* 1, 697–700.
- Nam, Y.S., Yoon, J.J., Park, T.G., 2000. A novel fabrication method of macroporous biodegradable polymer scaffolds using gas foaming salt as a porogen additive. *J. Biomed. Mater. Res.* 53, 1–7.
- Nasr, M., Awad, G.A.S., Mansour, S., Al Shamy, A., Mortada, N.D., 2013. Hydrophilic versus hydrophobic porogens for engineering of poly(lactide-co-glycolide) microparticles containing risedronate sodium. *Pharm. Dev. Technol.* 18, 1078–1088.
- Nasr, M., Awad, G.A.S., Mansour, S., Taha, I., Al Shamy, A., Mortada, N.D., 2011. Different modalities of NaCl osmogen in biodegradable microspheres for bone deposition of risedronate sodium by alveolar targeting. *Eur. J. Pharm. Biopharm.* 79, 601–611.
- Ni, R., Muenster, U., Zhao, J., Zhang, L., Becker-Pelster, E.M., Rosenbruch, M., Mao, S.R., 2017. Exploring polyvinylpyrrolidone in the engineering of large porous PLGA microparticles via single emulsion method with tunable sustained release in the lung: In vitro and in vivo characterization. *J. Control. Release* 249, 11–22.
- Nie, L., Zhang, G.H., Hou, R.X., Xu, H.P., Li, Y.P., Fu, J., 2015. Controllable promotion of chondrocyte adhesion and growth on PVA hydrogels by controlled release of TGF- $\beta$ 1 from porous PLGA microspheres. *Colloid Surface B* 125, 51–57.
- Nihant, N., Schugens, C., Grandfils, C., Jerome, R., Teyssie, P., 1994. Polylactide microparticles prepared by double emulsion/evaporation technique .1. Effect of primary emulsion stability. *Pharm Res-Dordr* 11, 1479–1484.
- Nihant, N., Schugens, C., Grandfils, C., Jerome, R., Teyssie, P., 1995. Polylactide microparticles prepared by double emulsion-evaporation .2. Effect of the poly(lactide-co-glycolide) composition on the stability of the primary and secondary emulsions. *J. Colloid Interf. Sci.* 173, 55–65.
- Niu, X.M., Zou, W.W., Liu, C.X., Zhang, N., Fu, C.H., 2009. Modified nanoprecipitation method to fabricate DNA-loaded PLGA nanoparticles. *Drug Dev. Ind. Pharm.* 35, 1375–1383.
- Oh, Y.J., Lee, J., Seo, J.Y., Rhim, T., Kim, S.H., Yoon, H.J., Lee, K.Y., 2011. Preparation of budesonide-loaded porous PLGA microparticles and their therapeutic efficacy in a murine asthma model. *J. Control. Release* 150, 56–62.
- Paik, D.H., Choi, S.W., 2014. Entrapment of protein using electrosprayed poly(D,L-lactide-co-glycolide) microspheres with a porous structure for sustained release. *Macromol. Rapid Commun.* 35, 1033–1038.
- Park, J.H., Han, C.M., Lee, E.J., Kim, H.W., 2016. Preparation of highly monodispersed porous-channelled poly(caprolactone) microspheres by a microfluidic system. *Mater. Lett.* 181, 92–98.
- Park, K., Skidmore, S., Hadar, J., Garner, J., Park, H., Otte, A., Soh, B.K., Yoon, G., Yu, D. J., Yun, Y., Lee, B.K., Jiang, X.H., Wang, Y., 2019. Injectable, long-acting PLGA formulations: analyzing PLGA and understanding microparticle formation. *J. Control. Release* 304, 125–134.
- Park, T.G., Cohen, S., Langer, R., 1992. Poly(L-lactic acid) pluronic blends - characterization of phase-separation behavior, degradation, and morphology and use as protein-releasing matrices. *Macromolecules* 25, 116–122.
- Pawłowski, S., Nayak, N., Meireles, M., Portugal, C.A.M., Velizarov, S., Crespo, J.G., 2018. CFD modelling of flow patterns, tortuosity and residence time distribution in monolithic porous columns reconstructed from X-ray tomography data. *Chem. Eng. J.* 350, 757–766.
- Pistel, K.F., Kissel, T., 2000. Effects of salt addition on the microencapsulation of proteins using W/O/W double emulsion technique. *J. Microencapsul.* 17, 467–483.
- Qu, M.Y., Liao, X.L., Jiang, N., Sun, W.J., Xiao, W.Q., Zhou, X.W., Khademhosseini, A., Li, B., Zhu, S.S., 2021. Injectable open-porous PLGA microspheres as cell carriers for cartilage regeneration. *J. Biomed. Mater. Res. A* 109, 2091–2100.
- Qutachi, O., Vetsch, J.R., Gill, D., Cox, H., Scurr, D.J., Hofmann, S., Müller, R., Quirk, R. A., ShakeSheff, K.M., Rahman, C.V., 2014. Injectable and porous PLGA microspheres that form highly porous scaffolds at body temperature. *Acta Biomater.* 10, 5090–5098.
- Ravivarapu, H.B., Lee, H., DeLuca, P.P., 2000. Enhancing initial release of peptide from poly(D,L-lactide-co-glycolide) (PLGA) microspheres by addition of a porosigen and increasing drug load. *Pharm. Dev. Technol.* 5, 287–296.
- Reinhold, S.E., Desai, K.G.H., Zhang, L., Olsen, K.F., Schwendeman, S.P., 2012. Self-healing microencapsulation of biomacromolecules without organic solvents. *Angew. Chem. Int. Ed.* 51, 10800–10803.
- Reinhold, S.E., Schwendeman, S.P., 2013. Effect of polymer porosity on aqueous self-healing encapsulation of proteins in PLGA microspheres. *Macromol. Biosci.* 13, 1700–1710.
- Ren, S.K., Wang, C.N., Guo, L., Xu, C.C., Wang, Y., Sun, C.J., Cui, H.X., Zhao, X., 2021. Preparation and sustained-release performance of PLGA microcapsule carrier system. *Nanomaterials-Basel* 11, 1758.
- Rouquerol, J., Avnir, D., Fairbridge, C.W., Everett, D.H., Haynes, J.H., Pernicone, N., Ramsay, J.D.F., Sing, K.S.W., Unger, K.K., 1994. Recommendations for the characterization of porous solids. *Pure Appl. Chem.* 66, 1739–1758.
- Scheiner, K.C., Maas-Bakker, R.F., van Steenberg, M.J., Schwendeman, S.P., Hennink, W.E., Kok, R.J., 2021. Post-loading of proangiogenic growth factors in PLGA microspheres. *Eur. J. Pharm. Biopharm.* 158, 1–10.
- Scheler, S., 2014. The polymer free volume as a controlling factor for drug release from poly(lactide-co-glycolide) microspheres. *J. Appl. Polym. Sci.* 131.
- Schiller, L.R., Emmett, M., Santaana, C.A., Fordtran, J.S., 1988. Osmotic effects of polyethylene-glycol. *Gastroenterology* 94, 933–941.
- Schlicher, E.J.A.M., Postma, N.S., Zuidema, J., Talsma, H., Hennink, W.E., 1997. Preparation and characterisation of poly(D,L-lactic-co-glycolic acid) microspheres containing desferrioxamine. *Int. J. Pharmaceut* 153, 235–245.

- Schugens, C., Laruelle, N., Nihant, N., Grandfils, C., Jerome, R., Teyssie, P., 1994. Effect of the emulsion stability on the morphology and porosity of semicrystalline poly L-lactide microparticles prepared by W/O/W double emulsion-evaporation. *J. Control. Release* 32, 161–176.
- Schutzman, R., Shi, N.Q., Olsen, K.F., Ackermann, R., Tang, J., Liu, Y.Y., Hong, J.K.Y., Wang, Y., Qin, B., Schwendeman, A., Schwendeman, S.P., 2023. Mechanistic evaluation of the initial burst release of leuprolide from spray-dried PLGA microspheres. *J. Control. Release* 361, 297–313.
- Schwendeman, S.P., 2005. *Methods for Encapsulation of Biomacromolecules in Polymers*, WO2005117942A2.
- Schwendeman, S.P., Shah, R.B., Bailey, B.A., Schwendeman, A.S., 2014. Injectable controlled release depots for large molecules. *J. Control. Release* 190, 240–253.
- Sediq, A.S., Waasdorp, S.K.D., Nejadnik, M.R., van Beers, M.M.C., Meulenaar, J., Verrijck, R., Jiskoot, W., 2017. Determination of the porosity of PLGA microparticles by tracking their sedimentation velocity using a flow imaging microscope (FlowCAM). *Pharm Res-Dordr* 34, 1104–1114.
- Shah, R.B., Schwendeman, S.P., 2014. A biomimetic approach to active self-microencapsulation of proteins in PLGA. *J. Control. Release* 196, 60–70.
- Sharma, A., Vaghasiya, K., Verma, R.K., 2016. Inhalable microspheres with hierarchical pore size for tuning the release of biotherapeutics in lungs. *Micropor Mesopor Mat.* 235, 195–203.
- Shi, X.D., Cui, L.G., Sun, H., Jiang, N., Heng, L.P., Zhuang, X.L., Gan, Z.H., Chen, X.S., 2019. Promoting cell growth on porous PLA microspheres through simple degradation methods. *Polym Degrad Stabil* 161, 319–325.
- Shi, X.D., Sun, L., Jiang, J., Zhang, X.L., Ding, W.J., Gan, Z.H., 2009. Biodegradable polymeric microcarriers with controllable porous structure for tissue engineering. *Macromol. Biosci.* 9, 1211–1218.
- Shi, X.D., Sun, P.J., Gan, Z.H., 2018. Preparation of porous polylactide microspheres and their application in tissue engineering. *Chin. J. Polym. Sci.* 36, 712–719.
- Si, W., Yang, Q.Q., Zong, Y., Ren, G.B., Zhao, L., Hong, M.H., Xin, Z., 2021. Toward understanding the effect of solvent evaporation on the morphology of PLGA microspheres by double emulsion method. *Ind. Eng. Chem. Res.* 60, 9196–9205.
- Siepmann, J., Elkharraz, K., Siepmann, F., Klose, D., 2005. How autocatalysis accelerates drug release from PLGA-based microcarriers: a quantitative treatment. *Biomacromolecules* 6, 2312–2319.
- Sodha, S., Gupta, P., 2023. PLGA and PEG based porous microparticles as vehicles for pulmonary somatropin delivery. *Eur. J. Pharm. Biopharm.* 191, 150–157.
- Sophocleous, A.M., Desai, K.G.H., Mazzara, J.M., Tong, L., Cheng, J.X., Olsen, K.F., Schwendeman, S.P., 2013. The nature of peptide interactions with acid end-group PLGAs and facile aqueous-based microencapsulation of therapeutic peptides. *J. Control. Release* 172, 662–670.
- Su, X., Gupta, I., Jonnalagadda, U.S., Kwan, J.J., 2020. Complementary effects of porosity and stabilizer on the structure of hollow porous poly(lactide-co-glycolic acid) microparticles. *ACS Appl. Polym. Mater.* 2, 3696–3703.
- Su, Y., Zhang, B.L., Sun, R.W., Liu, W.F., Zhu, Q.B., Zhang, X., Wang, R.R., Chen, C.P., 2021. PLGA-based biodegradable microspheres in drug delivery: recent advances in research and application. *Drug Deliv.* 28, 1397–1418.
- Sun, L., Zhou, S.B., Wang, W.J., Li, X.H., Wang, J.X., Weng, J., 2009. Preparation and characterization of porous biodegradable microspheres used for controlled protein delivery. *Colloid Surface A* 345, 173–181.
- Takai, C., Hotta, T., Shiozaki, S., Matsumoto, S., Fukui, T., 2011. Key techniques to control porous microsphere morphology in S/O/W emulsion system. *Colloid Surface A* 373, 152–157.
- Tang, J., Chen, J.Y., Liu, J., Luo, M., Wang, Y.J., Wei, X.W., Gao, X., Wang, B.L., Liu, Y.B., Yi, T., Tong, A.P., Song, X.R., Xie, Y.M., Zhao, Y.L., Xiang, M.L., Huang, Y., Zheng, Y., 2012. Calcium phosphate embedded PLGA nanoparticles: a promising gene delivery vector with high gene loading and transfection efficiency. *Int. J. Pharmaceut* 431, 210–221.
- Thickett, S.C., Hamilton, E., Yogeswaran, G., Zetterlund, P.B., Farrugia, B.L., Lord, M.S., 2019. Enhanced osteogenic differentiation of human fetal cartilage rudiment cells on graphene oxide-PLGA hybrid microparticles. *J. Funct. Biomater* 10.
- Ullah, A., Kim, C.M., Kim, G.M., 2017. Solvent effects on the porosity and size of porous PLGA microspheres using gelatin and PBS as porogens in a microfluidic flow-focusing device. *J. Nanosci. Nanotechnol* 17, 7775–7782.
- Ungaro, F., De Rosa, G., Miro, A., Quaglia, F., La Rotonda, M.I., 2006. Cyclodextrins in the production of large porous particles: development of dry powders for the sustained release of insulin to the lungs. *Eur. J. Pharm. Sci.* 28, 423–432.
- Ungaro, F., Giovino, C., Coletta, C., Sorrentino, R., Miro, A., Quaglia, F., 2010. Engineering gas-foamed large porous particles for efficient local delivery of macromolecules to the lung. *Eur. J. Pharm. Sci.* 41, 60–70.
- Varde, N.K., Pack, D.W., 2007. Influence of particle size and antacid on release and stability of plasmid DNA from uniform PLGA microspheres. *J. Control. Release* 124, 172–180.
- Vay, K., Scheler, S., Friess, W., 2010. New insights into the pore structure of poly(D,L-lactide-co-glycolide) microspheres. *Int. J. Pharmaceut* 402, 20–26.
- Wang, J., Wang, B.A., Schwendeman, S.P., 2002. Characterization of the initial burst release of a model peptide from poly(D,L-lactide-co-glycolide) microspheres. *J. Control. Release* 82, 289–307.
- Wang, L.C., Xie, Z.G., Bi, X.J., Wang, X., Zhang, A.Y., Chen, Z.Q., Zhou, J.Y., Feng, Z.G., 2006. Preparation and characterization of aliphatic/aromatic copolyesters based on 1,4-cyclohexanedicarboxylic acid. *Polym. Degrad Stabil* 91, 2220–2228.
- Wang, S.B., Guo, S.R., 2008a. Disodium norcantharidate-loaded poly( $\epsilon$ -caprolactone) microspheres II: modification of morphology and release behavior. *Int. J. Pharmaceut* 353, 15–20.
- Wang, S.B., Guo, S.R., 2008b. Formation mechanism and release behavior of poly( $\epsilon$ -caprolactone) microspheres containing disodium norcantharidate. *Eur. J. Pharm. Biopharm.* 69, 1176–1181.
- Wang, S.B., Guo, S.R., Cheng, L., 2008. Disodium norcantharidate loaded poly( $\epsilon$ -caprolactone) microspheres I: preparation and evaluation. *Int. J. Pharmaceut* 350, 130–137.
- Wang, S.Y., Downing, G., Olsen, K.F., Sawyer, T.K., Cone, R.D., Schwendeman, S.P., 2023a. Aqueous remote loading of setmelanotide in poly(lactide-co-glycolic acid) microspheres for long-term obesity treatment. *J. Control. Release* 364, 589–600.
- Wang, S.Y., Shi, X.D., Gan, Z.H., Wang, F., 2015. Preparation of PLGA microspheres with different porous morphologies. *Chin. J. Polym. Sci.* 33, 128–136.
- Wang, X., Wenk, E., Hu, X., Castro, G.R., Meinel, L., Wang, X., Li, C., Merkle, H., Kaplan, D.L., 2007. Silk coatings on PLGA and alginate microspheres for protein delivery. *Biomaterials* 28, 4161–4169.
- Wang, Z.-Y., Zhang, X.-W., Ding, Y.-W., Ren, Z.-W., Wei, D.-X., 2023b. Natural biopolyester microspheres with diverse structures and surface topologies as micro-devices for biomedical applications. *Smart Mater. Med.* 4, 15–36.
- Washington, M.A., Swiner, D.J., Bell, K.R., Fedorchak, M.V., Little, S.R., Meyer, T.Y., 2017. The impact of monomer sequence and stereochemistry on the swelling and erosion of biodegradable poly(lactide-co-glycolic acid) matrices. *Biomaterials* 117, 66–76.
- Wei, Y., Wang, Y.X., Zhang, H.X., Zhou, W.Q., Ma, G.H., 2016. A novel strategy for the preparation of porous microspheres and its application in peptide drug loading. *J. Colloid Interf Sci.* 478, 46–53.
- Wen, K., Na, X., Yuan, M., Bazybek, N., Li, X., Wei, Y., Ma, G., 2022. Preparation of novel ropivacaine hydrochloride-loaded PLGA microspheres based on post-loading mode and efficacy evaluation. *Colloids Surf. B Biointerfaces* 210, 112215.
- Wischke, C., Schwendeman, S.P., 2008. Principles of encapsulating hydrophobic drugs in PLA/PLGA microparticles. *Int. J. Pharm.* 364, 298–327.
- Wischke, C., Schwendeman, S.P., 2012. Degradable polymeric carriers for parenteral controlled drug delivery. In: Siepmann, J., Siegel, R.A., Rathbone, M.J. (Eds.), *Fundamentals and Applications of Controlled Release Drug Delivery*. Springer, US, Boston, MA, pp. 171–228.
- Witschi, C., Doelker, E., 1998. Peptide degradation during preparation and in vitro release testing of poly(L-lactic acid) and poly(DL-lactic-co-glycolic acid) microparticles. *Int. J. Pharmaceut* 171, 1–18.
- Woodruff, M.A., Hutmacher, D.W., 2010. The return of a forgotten polymer—Polycaprolactone in the 21st century. *Prog. Polym. Sci.* 35, 1217–1256.
- Wu, D., Wang, C.H., Yang, J.B., Wang, H., Han, H.B., Zhang, A.J., Yang, Y., Li, Q.S., 2016. Improving the intracellular drug concentration in lung cancer treatment through the codelivery of doxorubicin and miR-519c mediated by porous PLGA microparticle. *Mol. Pharmaceut* 13, 3925–3933.
- Wu, J.Q., Ding, J.Q., Xiao, B.Y., Chen, D.L., Huang, D.L., Ma, P., Xiong, Z.C., 2022. A facile strategy for controlling porous PLGA microspheres via o/w emulsion method. *J. Polym. Res.* 29, 508.
- Xiong, B.Y., Chen, Y.X., Liu, Y., Hu, X.L., Han, H.B., Li, Q.S., 2021. Artesunate-loaded porous PLGA microsphere as a pulmonary delivery system for the treatment of non-small cell lung cancer. *Colloid Surface B* 206, 111937.
- Yang, M., Wang, Y.Z., 2024. D-BJH: the intrinsic model for characterizing the pore size distribution of porous materials. *Langmuir* 40, 20368–20378.
- Yang, Y., Bajaj, N., Xu, P., Ohn, K., Tsifansky, M.D., Yeo, Y., 2009. Development of highly porous large PLGA microparticles for pulmonary drug delivery. *Biomaterials* 30, 1947–1953.
- Yang, Y.Y., Chia, H.H., Chung, T.S., 2000a. Effect of preparation temperature on the characteristics and release profiles of PLGA microspheres containing protein fabricated by double-emulsion solvent extraction/evaporation method. *J. Control. Release* 69, 81–96.
- Yang, Y.Y., Chung, T.S., Bai, X.L., Chan, W.K., 2000b. Effect of preparation conditions on morphology and release profiles of biodegradable polymeric microspheres containing protein fabricated by double-emulsion method. *Chem. Eng. Sci.* 55, 2223–2236.
- Yang, Y.Y., Chung, T.S., Ng, N.P., 2001. Morphology, drug distribution, and in vitro release profiles of biodegradable polymeric microspheres containing protein fabricated by double-emulsion solvent extraction/evaporation method. *Biomaterials* 22, 231–241.
- Yeo, Y., Park, K.N., 2004. Control of encapsulation efficiency and initial burst in polymeric microparticle systems. *Arch. Pharm. Res.* 27, 1–12.
- Yoo, J., Won, Y.Y., 2020. Phenomenology of the initial burst release of drugs from PLGA microparticles. *ACS Biomater Sci. Eng.* 6, 6053–6062.
- Yuan, Y., Shi, X.D., Gan, Z.H., Wang, F.S., 2018. Modification of porous PLGA microspheres by poly-L-lysine for use as tissue engineering scaffolds. *Colloid Surface B* 161, 162–168.
- Zech, J., Leisz, S., Gattel, B., Syrowatka, F., Greiner, A., Strauss, C., Knolle, W., Scheller, C., Mader, K., 2020. Electrospun Nimodipine-loaded fibers for nerve regeneration: development and in vitro performance. *Eur. J. Pharm. Biopharm.* 151, 116–126.
- Zhang, C., Zhou, Z.H., Liu, W.J., Huang, T.L., Zhao, Y.M., Chen, P., Zhou, Z.W., Wang, D., Yi, M.L., Fang, J.J., 2021. Preparation and characterization of poly(L-lactide-co-glycolide-co- $\epsilon$ -caprolactone) Porous microspheres. *J. Macromol. Sci. B* 60, 313–323.
- Zhang, C.H., Bodmeier, R., 2024. Porous PLGA microparticles prepared with nanosized/micronized sugar particles as porogens. *Int. J. Pharmaceut* 660, 124329.
- Zhang, C.Q., Yang, L., Wan, F., Bera, H., Cun, D.M., Rantanen, J., Yang, M.S., 2020a. Quality by design thinking in the development of long-acting injectable PLGA/PLA-based microspheres for peptide and protein drug delivery. *Int J Pharmaceut* 585, 119441.

- Zhang, J.X., Zhu, K.J., 2004. An improvement of double emulsion technique for preparing bovine serum albumin-loaded PLGA microspheres. *J. Microencapsul.* 21, 775–785.
- Zhang, S., Wu, D., Zhou, L.P., 2020b. Characterization of controlled release microspheres using FIB-SEM and image-based release prediction. *AAPS PharmSciTech* 21.
- Zhang, T.Z., Zhang, Q.Y., Chen, J.S., Fang, K., Dou, J., Gu, N., 2014. The controllable preparation of porous PLGA microspheres by the oil/water emulsion method and its application in 3D culture of ovarian cancer cells. *Colloid Surface A* 452, 115–124.
- Zhang, X.F., Qin, L., Su, J., Sun, Y., Zhang, L., Li, J.Q., Beck-Broichsitter, M., Muenster, U., Chen, L., Mao, S.R., 2020c. Engineering large porous microparticles with tailored porosity and sustained drug release behavior for inhalation. *Eur. J. Pharm. Biopharm.* 155, 139–146.
- Zhang, Y., Schwendeman, S.P., 2012. Minimizing acylation of peptides in PLGA microspheres. *J. Control. Release* 162, 119–126.
- Zhang, Y., Wischke, C., Mittal, S., Mitra, A., Schwendeman, S.P., 2016. Design of controlled release PLGA microspheres for hydrophobic fenretinide. *Mol Pharmaceut* 13, 2622–2630.
- Zhou, J., Hirota, K., Ackermann, R., Walker, J., Wang, Y., Choi, S., Schwendeman, A., Schwendeman, S.P., 2018. Reverse engineering the 1-month lupron Depot®. *AAPS J.* 20, 105.
- Zhu, H.J., Chen, H.B., Zeng, X.W., Wang, Z.Y., Zhang, X.D., Wu, Y.P., Gao, Y.F., Zhang, J. X., Liu, K.W., Liu, R.Y., Cai, L.T., Mei, L., Feng, S.S., 2014. Co-delivery of chemotherapeutic drugs with vitamin E TPGS by porous PLGA nanoparticles for enhanced chemotherapy against multi-drug resistance. *Biomaterials* 35, 2391–2400.
- Zhu, L., Li, M., Liu, X., Du, L., Jin, Y., 2017. Inhalable oridonin-loaded poly(lactic-co-glycolic)acid large porous microparticles for in situ treatment of primary non-small cell lung cancer. *Acta Pharm. Sin. B* 7, 80–90.
- Zolnik, B.S., Burgess, D.J., 2007. Effect of acidic pH on PLGA microsphere degradation and release. *J. Control. Release* 122, 338–344.
- Zolnik, B.S., Leary, P.E., Burgess, D.J., 2006. Elevated temperature accelerated release testing of PLGA microspheres. *J. Control. Release* 112, 293–300.